Precambrian Research 340 (2020) 105527

Contents lists available at ScienceDirect

Precambrian Research

journal homepage: www.elsevier.com/locate/precamres

Tectonomagmatic evolution of the Sveconorwegian orogen recorded in the chemical and isotopic compositions of 1070–920 Ma granitoids

Anette Granseth[a,*], Trond Slagstad[b], Nolwenn Coint[b], Nick M.W. Roberts[c], Torkil S. Røhr[b], Bjørn Eske Sørensen[a]

[a] Department of Geoscience and Petroleum, Norwegian University of Science and Technology, S. P. Andersens Veg 15a, 7031 Trondheim, Norway
[b] Geological Survey of Norway, 7491 Trondheim, Norway
[c] Geochronology and Tracers Facility, British Geological Survey, Nottingham NG12 5GG, UK

ARTICLE INFO

Keywords:
Sveconorwegian orogen
Mafic underplating
Granitoid magmatism
Geochemistry
Sm-Nd isotopes
Trace element modelling

ABSTRACT

The Sveconorwegian Province in Southern Norway and Sweden hosts at least four granitoid suites, representing apparently continuous magmatism at the SW margin of the Fennoscandian Shield between 1070 and 920 Ma. This study presents a compilation of published and new zircon LA-ICP-MS U-Pb geochronology, whole-rock and zircon geochemistry and Sm-Nd isotope data for the granitoid suites and demonstrates the granitoids' ability to record changes in the tectonomagmatic evolution of this orogenic Province. The Sirdal Magmatic Belt (SMB, ca. 1070–1010 Ma) represents the earliest magmatism, west in the Province, followed by two hornblende-biotite granitoid suites (HBG, ca. 1000–920 Ma) and the Flå–Iddefjord–Bohus suite (FIB, ca. 925 Ma), in central and eastern parts of the Province, respectively. The SMB and the HBG bodies located outside of the SMB (referred to as HBGout) are chemically similar, whereas the HBG bodies located in the same region as the SMB (referred to as HBGin) are more ferroan, enriched in incompatible elements and have higher zircon saturation temperatures. Isotopically, the SMB and both HBG suites fall on an evolutionary trend from widespread 1.5 Ga crust in the region, suggesting this was the dominant crustal contribution to magmatism. The FIB suite is more peraluminous, rich in inherited zircon, and has isotopic compositions suggesting a more evolved source than both the HBG suites and the SMB. Trace element modelling shows that the SMB and HBGout suites could have formed by 50% partial melting of 1.5 Ga crust, whereas 5–10% remelting of the dehydrated and depleted SMB residue accounts for the geochemical composition of the HBGin suite. The available data suggest a scenario where the 1.5 Ga lower crust underwent melting due to long-lived mafic underplating giving rise to the SMB suite. After ca. 1000 Ma, regional-scale extension may have led to more widespread mafic underplating causing remelting of the residue following SMB melt extraction, forming the HBGin suite, with lower-crustal melting farther east forming the HBGout suite. Changes in melt composition over this 150 Myr time interval may thus be ascribed to an evolving melt source rather than fundamental changes in tectonic regime. Deep continental subduction at ca. 990 Ma, east in the orogen, provided an isotopically evolved crustal source for the FIB suite. The data underline the difference in tectonic processes across the orogen, with long-lived, high temperatures in the western and central parts and colder, high-pressure events in the eastern parts of the orogen.

1. Introduction

Granitoid rocks are the most common magmatic rocks found in the continental crust. They form in various tectonic settings and preserve evidence of the source and processes that lead to formation of continental crust by growth and reworking (e.g. Goodge and Vervoort, 2006, Zhao et al., 2008; Zhao et al., 2016). The evidence is stored in the geochemical and isotopic composition of the granitoids and tracking the variations through time and space gives an indirect view into the source and associated magmatic processes, in turn recording the region's geodynamic history.

The western and central parts of the late Mesoproterozoic Sveconorwegian Province in southwestern Fennoscandia was characterised by voluminous granitoid and minor mafic magmatism (e.g. Andersen et al., 2002, 2009; Coint et al., 2015; Eliasson and Schöberg, 1991; Slagstad et al., 2018; Vander Auwera et al., 2003). The granitoid magmatism was continuous between 1070 and 920 Ma and has been subdivided into two periods based on geochronological and

* Corresponding author.
E-mail address: anettegranseth@gmail.com (A. Granseth).

https://doi.org/10.1016/j.precamres.2019.105527
Received 29 August 2019; Received in revised form 25 October 2019; Accepted 1 November 2019
Available online 04 November 2019

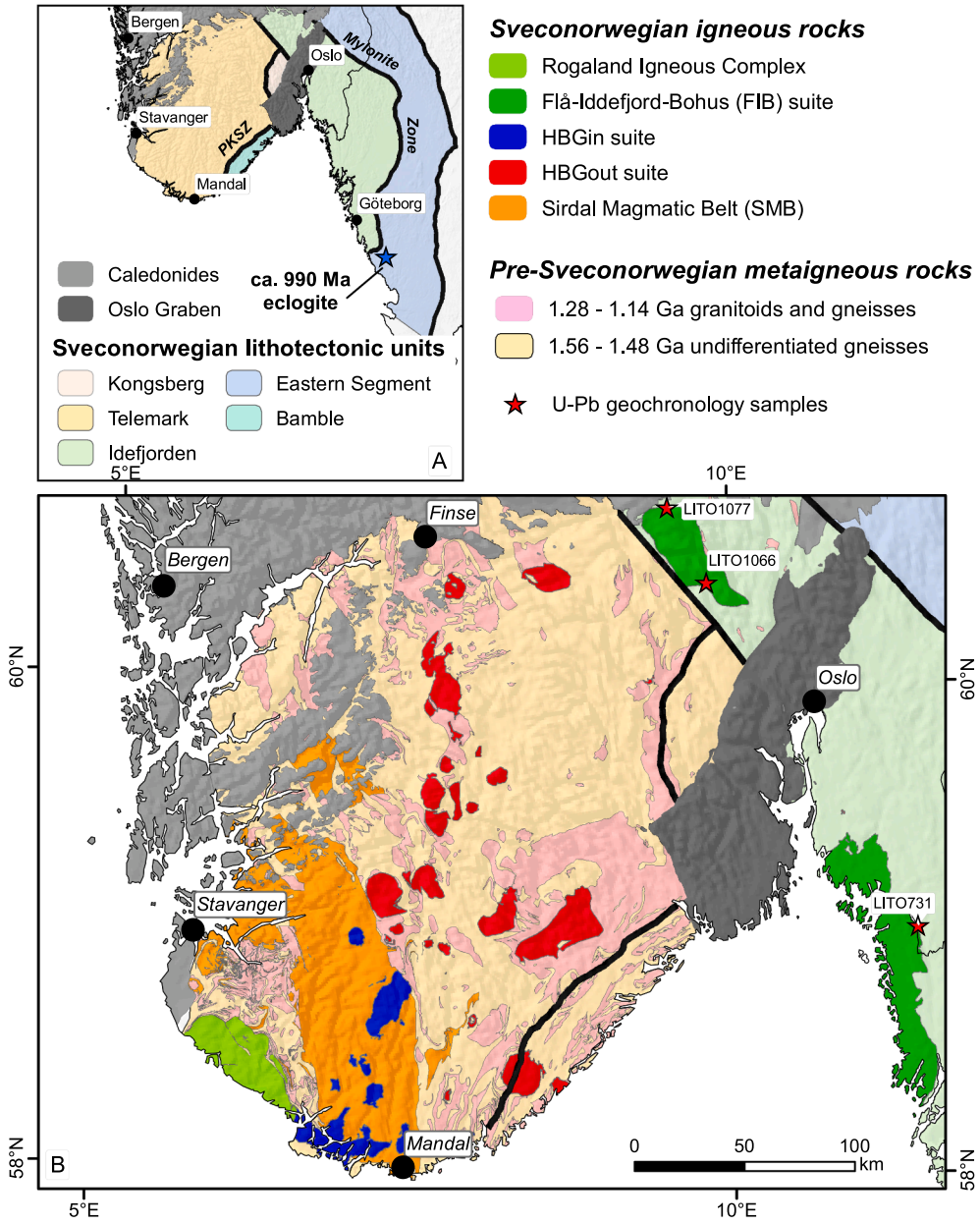

Fig. 1. (A) Main lithotectonic units of the Sveconorwegian Province, separated by shear zones. The location of ca. 990 Ma eclogite in the Eastern Segment is indicated. (B) A more detailed map of the western and central parts of the Sveconorwegian Province highlighting various igneous units discussed in the text. The HBGin, HBGout and FIB suites represent a new tripartite subdivision proposed here for what was originally a single suite of "post-orogenic granitoids", typically referred to as the hornblende-biotite granitoid (HBG) suite. The colour scheme of the granitoid suites follows the colour scheme used for the plots in this paper.

geochemical data. The Sirdal Magmatic Belt (SMB) was emplaced in the west of the orogen between 1070 and 1010 Ma, followed by emplacement of a hornblende-biotite-bearing granitoid (HBG) suite in western and central parts of the orogen between 1000 and 920 Ma (Fig. 1). Numerous geochemical studies have been conducted in the Sveconorwegian Province focussing on a subset of these granitoid suites (e.g. Andersen et al., 2009b, Bingen et al., 1993, Vander Auwera et al., 2003). Falkum (1982), Bingen (1989) and Bingen et al. (1993) identified and documented an elongate body of porphyritic granodiorite rich in alkali feldspar phenocrysts in the western parts of the Province, which they referred to as the Feda augen gneiss. This augen gneiss was later dated to ca. 1051 Ma by Bingen and Van Breemen (1998), and interpreted to represent a short-lived magmatic event in a subduction-related geodynamic regime. Since the early 2000 s, mapping by the Geological Survey of Norway (NGU) has shown that the extent of these rocks was significantly larger, and the Feda augen gneiss is now considered part of the much larger SMB suite (Slagstad et al., 2013). The presence of older crustal components residing in the Sveconorwegian lower crust plays an important role in petrogenetic models proposed for the HBG suites (e.g. Andersen et al., 2009b; Vander Auwera et al., 2011). These crustal components have been invoked to explain the spread in trace element and isotopic composition of HBG magmas. Vander Auwera et al., 2003, 2011 interpreted the continuous compositional trend of the HBGs to be a result of partial melting and fractional crystallisation of previously underplated basalts formed in a convergent margin setting and that the source(s) of the HBG suites and Feda (now SMB) suite were variably contaminated by these components. Alternatively, Andersen et al. (2001, 2009b) argued that the HBG magmas resulted from imperfect mixing between anatectic and mafic, mantle-derived melts. They identified two crustal components residing in the

Table 1
. Overview of the compiled data and data from this study. Crossed symbols indicate that data exist for the suite, either as whole-rock geochemistry or isotope data or as both.

	No. of data		Suites			
Refs.	Whole-rock	Nd	SMB	HBGin	HBGout	FIB
Bingen (1989)	27		X			
Bingen et al. (1993)	15	10	X			
Slagstad et al. (2013)	47		X			
Stormoen (2015)	19		X			
Bogaerts et al. (2003)	43	13		X		
Menuge (1988)		6		X		
Andersen (1997)		13			X	
Pedersen and Maaløe (1990)	16					X
Welin (1994)		3				X
Pedersen and Konnerup-Madsen (2000)	12		X		X	
Vander Auwera et al. (2003)	53	17		X	X	
Andersen et al. (2009b)	22			X	X	
Andersen et al. (2001)		48		X	X	X
This study	**309**	**30**	**X**	**X**	**X**	**X**
Total	**563**	**140**				

lower crust based on trace elements and Lu-Hf systematics of zircons: a ca. 1.7 Ga Paleoproterozoic component indistinguishable from the ca. 1.8 Ga Transscandinavian Intrusive Belt lithologies (Andersen et al., 2009a) and an early Mesoproterozoic ca. 1.5 Ga component, similar to the ca. 1.5 Ga metarhyolites of Telemark.

Today, our understanding of the tectonomagmatic and -metamorphic evolution of the Province has changed significantly since it became apparent that the Sveconorwegian magmatism was more widespread and protracted than previously thought and temporally linked to high-grade metamorphism (Slagstad et al., 2018b). This increased knowledge and a larger geochronological and geochemical/isotopic database allow the magmatic evolution of the orogen and its links to tectonic evolution to be reassessed. Here, we present new geochronological, whole-rock geochemical and Sm–Nd isotope data, together with a compilation of already published data for the granitoid rocks from the whole Sveconorwegian Province (Table 1). We have subdivided the granitoids of the Sveconorwegian Province into four suites based on their known field relationships, geochronology, and distinctive geochemical and isotopic features, and this subdivision forms a basis for discussing the suites' petrogenesis, source(s) and genetic relationships. Based on the petrogenetic interpretations, we outline a tectonic evolution for the orogen. The results of this study show that the geochemical and isotopic compositions of granitoid rocks may serve as excellent recorders of petrogenesis and underlying tectonic processes.

2. Geological background

The Sveconorwegian Province spans from SW Norway to the western parts of Sweden, bordered by Caledonian nappes to the north and the Sveconorwegian front to the east. The Province consists of five lithotectonic units that are bounded by major, probably crustal-scale shear zones with late Palaeo- through Mesoproterozoic protoliths that progressively young from east to west (Fig. 1). The Eastern Segment is made up of 1.8–1.65 Ga granitoids of the Transscandinavian Intrusive Belt (TIB) (Högdahl et al., 2004). The Nd isotope data for the TIB show evidence for reworking of older Svecofennian crust with minor juvenile additions (Andersson, 1997). The Idefjorden lithotectonic unit consists of plutonic, volcanic and sedimentary complexes that formed between 1660 and 1520 Ma (Brewer et al., 1998, Åhäll and Connelly, 2008). The Kongsberg and correlated Bamble lithotectonic units comprise orthogneisses of plutonic and volcanic origin that formed between ca. 1650 and 1480 Ma, with associated metasedimentary successions (Bingen and Viola, 2018, Nijland et al., 2014, Slagstad et al., submitted.). The Telemark lithotectonic unit consists of ca. 1585–1480 Ma volcanic and plutonic suites (Bingen et al., 2005, Roberts et al., 2013, Slagstad et al., submitted.), intruded by a bimodal suite at ca. 1.28–1.20 Ga (Bingen et al., 2002, Brewer et al., 2004, Pedersen et al., 2009, Slagstad et al., submitted.). The 1.5 Ga suite is generally calc-alkaline, whereas Nd isotope data indicate relatively juvenile values for both the 1.5 Ga (between + 1.0 to + 5.3) and the 1.28–1.2 Ga (between +0.7 to +6.3) suites (Brewer and Menuge, 1998, Brewer et al., 2004). The Sveconorwegian metamorphic evolution is characterised by geographically and temporally discrete events between 1140 and 920 Ma, that variably reworked the pre-Sveconorwegian crust (Bingen et al., 2008, Slagstad et al., 2017). High-grade metamorphism in the Bamble and Kongsberg lithotectonic units at ca. 1140 Ma is typically taken as the onset of Sveconorwegian orogenesis (Bingen et al., 2008). Notably, sedimentation was active in the Telemark lithotectonic unit until at least 1110 Ma (Spencer et al., 2014), with the first high-grade metamorphic events recorded at ca. 1070 Ma (Blereau et al., 2019; Slagstad et al., 2018), i.e., ca. 70 Myr after the onset in Bamble–Kongsberg. The Bamble–Kongsberg lithotectonic units are separated from the structurally lower Telemark lithotectonic unit by a high-strain zone (e.g. Scheiber et al., 2015); however, the timing of movement along this shear zone(s) and of final emplacement onto Telemark is unknown. Continued sedimentation until 1110 Ma in Telemark and lack of high-grade metamorphism before ca. 1070 Ma, suggest that final westward thrusting may have taken place long after higher-grade metamorphism in Bamble–Kongsberg. The distribution of metamorphic rocks in the Telemark lithotectonic unit is highly variable, with large tracts recording only low-grade Sveconorwegian metamorphism, in contrast to the SW part of the unit, in Rogaland, which records high-T to ultrahigh-T metamorphism apparently continuously between ca. 1070 and 920 Ma (Drüppel et al., 2013; Slagstad et al., 2018). The Sveconorwegian metamorphic record from the Idefjorden lithotectonic unit is sparse, but records high-pressure metamorphism at ca. 1050 Ma, probably related to internal thrusting in the unit, as well as a later ca. 1025 Ma high-pressure event (Söderlund et al., 2008). High-pressure, eclogite-facies metamorphism is well documented in the Eastern Segment at ca. 990 Ma (Möller et al., 2015, Tual et al., 2017), probably reflecting westward subduction of the Eastern Segment under the Idefjorden lithotectonic unit (Brueckner, 2009) along the Mylonite Zone, underlining the contrasting high-pressure and high-temperature metamorphic histories in the eastern and western parts of the orogen, respectively (e.g. Falkum and Petersen, 1980). The area studied here generally corresponds to the western and central parts of the orogen, where the geological record appears to suggest a tectonic evolution characterised by long-lived, high-temperature metamorphism, lower-crustal melting and emplacement of voluminous granites and minor, sporadic mafic magmatism between 1070 and 920 Ma (Slagstad et al., 2018b).

The granitoid rocks studied here are located largely in the Telemark, Bamble and Kongsberg lithotectonic units, with one late-orogenic granitoid suite in Idefjorden, and represent 150 million years of apparently continuous magmatism. The first significant Sveconorwegian magmatism starts at ca. 1070 Ma with emplacement of the early phases of the Sirdal Magmatic Belt (SMB suite) between 1070 and 1010 Ma in Telemark. The SMB suite was emplaced during regional compression (Henderson and Ihlen, 2004, Stormoen, 2015) that resulted in N-S elongated sheeted intrusions (Coint et al., 2015; Slagstad et al., 2018). Molybdenum-bearing granite (Mo-granite) and a nickel-bearing diorite (Ni-diorite) are emplaced coevally to the SMB magmatism at 1036 ± 6 Ma (Bingen et al., 2015) and 1025 ± 13 Ma (Slagstad et al., 2018b), respectively. After a lull in magmatic activity between ca. 1010

and 1000 Ma, magmatic activity picks up again with the Telemark-wide emplacement of hornblende-biotite-bearing granitoids (HBGs) (Vander Auwera et al., 2003, 2014), that partially crosscut the SMB suite and have more irregular, circular shapes, suggesting a change in stress regime. HBGs that intrude the older SMB suite have been termed HBGin in this study, while HBGs intruding mainly ca. 1.5 and 1.25 Ga metaigneous host rocks east of the SMB are referred to as HBGout (see Fig. 1). An AMCG (anorthosite-mangerite-charnockite-granite) complex, termed the Rogaland Igneous Complex (RIC), intruded the westernmost part of the Province. Zircon U–Pb data suggest the complex crystallised at ca. 930–920 Ma (Schärer et al., 1996; Slagstad et al., 2018b; Vander Auwera et al., 2011), comparatively late in the orogenic history. However, dating of high-alumina orthopyroxene megacrysts from the anorthosite, interpreted to have crystallised from basaltic melt at the Moho and comagmatic with the anorthositic plagioclase cumulate, has yielded an age of ca. 1040 Ma (Bybee et al., 2014), similar to the age of SMB magmatism. This age suggests that final emplacement at ca. 930 Ma may have been the last event in a protracted magmatic evolution, consistent with the duration of granitoid magmatism. Emplacement of the Flå-Iddefjord-Bohus (FIB) suite intrudes in the Idefjorden lithotectonic unit at ca. 925 Ma (928 ± 5 Ma; Bingen et al., 2008, ± 5 and 922 ± 5 Ma; Eliasson and Schöberg, 1991) marks the end of the granitoid magmatism in the Sveconorwegian Province.

3. Methods

3.1. Sample compilation

The data compilation consists of a total of 563 whole-rock major and trace element analyses and 140 whole-rock Sm-Nd isotopic analyses (Table 1). All four suites are referred to as granitoids, as these suites represents felsic fractionated melts and most likely lie in the continuum between 20% and 60% quartz and variable proportions of plagioclase and alkali feldspar. As discussed above, the HBGs have been subdivided into two suites in this study. The HBGin suite comprises plutons intruded in the older SMB suite and the HBGout suite constitutes plutons emplaced in a variety of host rocks east of the SMB. The collective term HBG has been used when referring to both the HBGin and HBGout suite.

3.2. U-Pb geochronology

3.2.1. Sample preparation

Zircons were separated by standard techniques including water table, heavy liquids, magnetic separation and final hand picking under a binocular microscope. The zircons were mounted in epoxy and polished to approximately half thickness, and cathodoluminescence (CL) images were obtained with a scanning electron microscope to reveal internal structures such as growth zoning and core-rim relationships.

3.2.2. LA-ICP-MS

LA–ICP–MS (Laser ablation Inductively Coupled Mass Spectrometry) analyses were conducted at the Geological Survey of Norway (NGU) on an ELEMENT XR single collector, high-resolution ICP–MS, coupled to a UP193–FX 193 nm short-pulse excimer laser ablation system from New Wave Research. The laser was set to ablate single, up to 60 µm-long lines, using a spot size of 20 or 15 µm, a repetition rate of 10 Hz and an energy corresponding to a fluence of 4–5 J/cm2. Each analysis included 30 s of background measurement followed by 30 s of ablation. The masses 202, 204, 206, 207, 208, 232 and 238 were measured. The reference material GJ–1 (Jackson et al., 2004) was used for correction of isotopic ratios, whereas 91500 (Wiedenbeck et al., 1995) and an in-house standard (OS–99–14; 1797 ± 3 Ma; Skår, 2002) were used to check precision and accuracy. The data were not corrected for common lead, but monitoring of the signal for 204 allowed exclusion of affected data from further calculations. The data were reduced using the GLITTER® software (van Achterbergh et al., 2001). The LA–ICP–MS analyses at NGU were conducted as part of the CAMOC (Centre for Advanced Mineral and Ore Characterisation) collaboration between NGU and the Department of Geoscience and Petroleum, Norwegian University of Science and Technology (NTNU).

3.3. Whole-rock major and trace element analyses

Samples were analysed by XRF at the Geological Survey of Norway (NGU) and were performed on fused lithium tetraborate discs for the major and minor elements, whereas the trace elements were determined on pressed powder pellets. REE (rare earth elements) and several trace elements (Nb, Hf, Ta, Th, U) were analysed by LA-ICP-MS following Flem et al. (2005), using the same glass discs from which XRF major element data were obtained.

3.4. Zircon trace element analyses

Trace element concentrations in zircon were determined at NGU on an ELEMENT XR single collector, high-resolution ICP–MS, coupled to a UP193–FX 193 nm short-pulse excimer laser ablation system from New Wave Research. The laser was operated at a frequency of 8 Hz, laser energy 4.0 J/cm^2 and a static spot size of 10 µm. Trace elements were measured in 300 M/ΔM (Low Resolution) mode. Background counts were measured for 40 s followed by 20 s laser ablation. For data reduction, the GLITTER® software package version 4.4.4 (van Achterbergh et al., 2001) was used. Concentrations were calibrated using Si^{29} as internal standard and NIST SRM 610 as external standard. To control the accuracy and precision of the analyses, NIST SRM 612 was analysed together with the samples. The concentrations of NIST SRM 610 and 612 were taken from Jochum et al. (2011).

3.5. Whole-rock Sm-Nd isotopes

Whole-rock Sm-Nd isotopes were analysed at the NERC Isotope Geosciences Laboratories (NIGL) at the British Geological Survey.

3.5.1. Dissolution and column chemistry

150–200 mg of sample was weighed into 15 ml Savillex teflon beakers and leached in 5 mls of 6 M HCl at 60 °C for 2 h. After discarding the leachate, the samples were washed and centrifuged twice in mQ water, dried and reweighed. 1-2mls of 2x quartz-distilled 16 M HNO_3 and 5–6 mls of 29 M HF were added, and the sample beakers were left closed on a hotplate at 140 °C overnight. After evaporating to dryness, a further 1–2 mls of HNO_3 were added, and the samples were left on the hotplate closed overnight. The samples were then converted to chloride form using 10 mls of Teflon-distilled HCl. The samples were then dissolved in ca. 2 ml of calibrated 2.5 M HCl in preparation for column chemistry, and centrifuged.

3.5.2. Separation of Nd from the bulk REE fraction

Sm and Nd were separated using 2mls of EICHROM LN-SPEC ion exchange resin packed into 10 ml Biorad Poly-Prep columns. The bulk REE fraction was dissolved in 200 Âµl of 0.2 M HCl and loaded onto the columns. La, Ce and Pr were eluted using a total of 14mls of 0.2 M HCl. Nd was collected in 3mls of 0.3 M HCl.

3.5.3. Mass spectrometry

Nd fractions were loaded onto one side of an outgassed double Re filament assembly using dilute HCl and analysed in a Thermo Scientific Triton mass spectrometer in multi-dynamic mode. Data are normalised

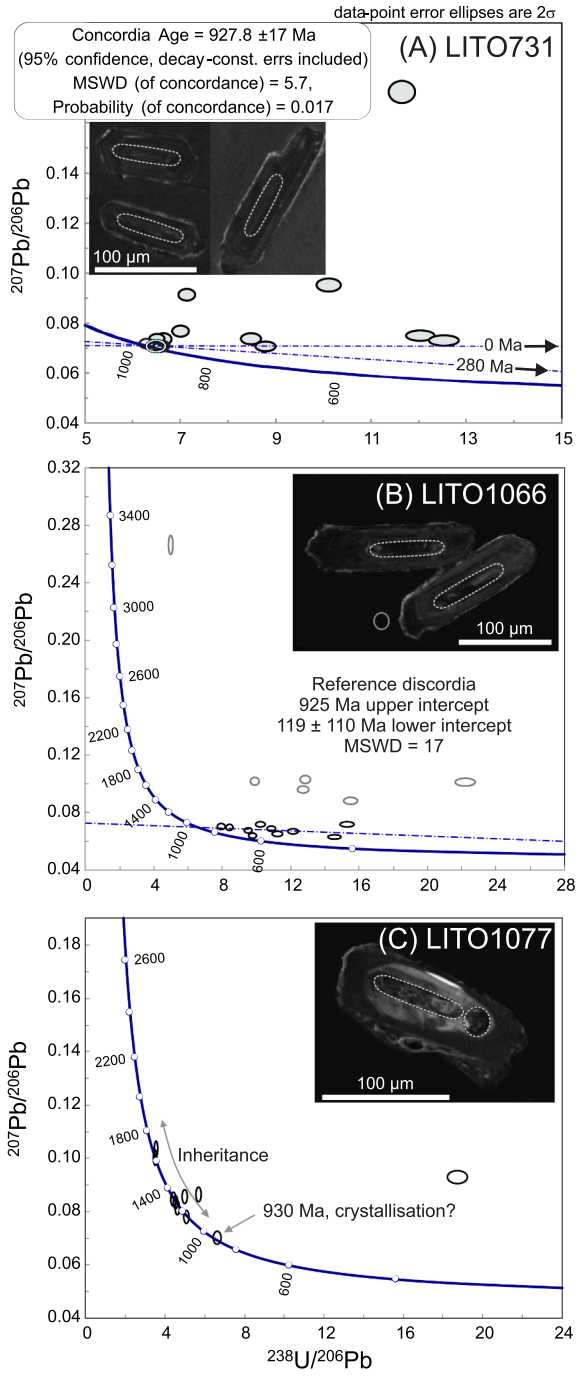

Fig. 2. Tera–Wasserburg plots presenting U–Pb zircon data from the FIB (Flå–Iddefjord–Bohus) granites. (A) Sample LITO731 from the Iddefjord granite. The concordia age of 928 ± 17 Ma is interpreted as the crystallisation age of the Iddefjord granite, similar to previously reported ages from pegmatites in the Bohus granite in Sweden – the southern extension of the Iddefjord granite. (B) Sample LITO1066 from the Flå granite. A reference discordia through the analyses with black ellipses, anchored at 925 Ma, yields and an MSWD of 17, suggesting significant geological scatter. (C) Sample LITO1077, also from the Flå granite, shows significant inheritance with a single analysis at ca. 930 Ma that may record crystallisation. Magmatic crystallisation is probably recorded by CL-dark, faintly zoned mantles that were generally too thin to analyse. Hatched domains represent laser-ablation lines.

to $^{146}Nd/^{144}Nd = 0.7219$. Five analyses of the La Jolla standard gave a value of 0.0.511842 ± 0.000008 (1-sigma). Results are quoted relative to a value of 0.511864 for this standard.

4. Results

4.1. Geochronology

Geochronological data are presented in Electronic Supplement 1.

4.1.1. Sample LITO731, Iddefjord granite

Sample LITO731 is a white–pink medium-grained granite and is generally massive with no foliation. It consists of approximately equal amounts of quartz, pink alkali feldspar and euhedral white plagioclase (norm: 28% quartz, 31% alkali feldspar, 36% plagioclase), with minor amounts of biotite. The zircons from this sample are 100–150 µm, prismatic and dark in CL (cathodoluminescence) with a faint oscillatory zoning suggesting a magmatic origin. Fifteen analyses from 15 grains show significant variations in U–Pb isotopic composition. Four near-concordant analyses yield a concordia age of 928 ± 17 Ma (MSWD = 5.7), with the other analyses displaying variable degrees of discordance (Fig. 2A). Calculated alpha doses (assuming 930 Ma age) from these zircons range from 3 to 11 × 10^{15} alpha-decay events per milligram, consistent with significant radiation damage (Murakami et al., 1991), and correlates well with $(La/Sm)_N$. Such a correlation has been shown to be consistent with loss of Pb and associated gain in LREE during fluid-mediated element mobility (Kirkland et al., 2018); however, the discordant analyses do not define anything that resembles a coherent discordia line, suggesting there are other, unresolved complexities in the dataset. Calculating discordia lines calculated from the concordant population and anchored at 280 Ma (age of nearby Oslo Rift) and present-day show that Pb-loss related to one or both events cannot explain the distribution of discordant analyses. We interpret the concordia age of 928 ± 17 Ma to date crystallisation of the Iddefjord granite, consistent with earlier dating of pegmatites (919 ± 5 Ma and 922 ± 5 Ma) from the Bohus granite in Sweden, the southern extension of the Iddefjord granite (Eliasson and Schöberg, 1991).

4.1.2. Sample LITO1066, Flå granite

Sample LITO1066 is a white–pink medium to coarse-grained granite (norm: 28% quartz, 31% alkali feldspar and 36% plagioclase). It is heterogeneous in appearance and has a foliation defined by the orientation of the mica. The sample displays an overall deformed appearance. The major mineralogy consists of white plagioclase, pink alkali feldspar and grey quartz of variable grain sizes, with minor amounts of biotite. The zircons from this sample are 100–200 µm, prismatic and dark in CL with a faint oscillatory zoning suggesting a magmatic origin, very similar to those from sample LITO731. Seventeen analyses were made from seventeen zircons in this sample. Most of the analyses are strongly discordant, but ten analyses fall close to a discordia anchored at 925 Ma (Fig. 2B), consistent with the much more precise age of 928 ± 3 Ma obtained by Bingen et al. (2008). The MSWD of this discordia is 17, suggesting significant geological scatter. Calculated alpha doses (assuming 925 Ma age) range from 3 to 10 × 10^{15} alpha-decay events per milligram, consistent with significant radiation damage, similar to sample LITO731.

4.1.3. Sample LITO1077, Flå granite

Sample LITO1077 is a fine-grained white–grey granite (norm: 32% quartz, 34% alkali feldspar and 30% plagioclase). The sample is homogeneous with randomly oriented black biotite. The zircons from this sample are 100–150 µm, stubby to prismatic with irregularly zoned cores surrounded by CL-dark, faintly zoned mantles. Considering the high-U composition of the Flå granite (Slagstad, 2008) and the appearance of analysed zircons from sample LITO1066 and sample LITO731 from the correlative Iddefjord granite, the CL-dark mantles most likely represent crystallisation of the granite. Unfortunately, the mantles were too thin to analyse. Six analyses of the cores are < 5% discordant and yield $^{207}Pb/^{206}Pb$ ages of ca. 1150, 1230, 1285, 1310, 1625 and 1690 Ma (Fig. 2C), interpreted to reflect inheritance in the

Table 2
Comparative geochemical and isotopic features of the four magmatic suites. Values are given as means with ranges in parentheses, unless otherwise is stated. The Eu anomaly, $(Eu/Eu^*)_N = Eu_N/(Sm_N \times Gd_N)^{0.5}$, is the ratio between the Eu content of the sample and Eu*, the theoretical Eu content based on interpolation of the neighbouring elements in the lanthanide series, Sm and Gd, normalised to their chondrite values after Taylor and McLennan (1985). REE, LREE and HREE fractionation indices are calculated with the normalisation values given by Taylor and McLennan (1985).

	SMB	HBGin	HBGout	FIB
# samples (n_{tot} = 563)	312	103	109	39
SiO_2 wt. %	69.4 (53.0–81.9)	64.5 (50.9–75.6)	69.1 (54.5–77.9)	70.7 (52.9–76.0)
K_2O wt. %	4.63 (0.197–9.64)	4.09 (2.28–5.9)	5.02 (1.05–6.81)	5.09 (2.99–5.98)
Na_2O wt. %	3.64 (2.06–10.0)	3.33 (2.28–5.3)	3.55 (1.5–5.12)	3.41 (2.3–4.67)
$K_2O + Na_2O$ wt. %	8.28 (6.3–14.0)	7.4 (5.06–9.4)	8.6 (5.6–10.1)	8.5 (5.8–9.5)
A/CNK	1.00 (0.69–1.16)	0.83 (0.62–1.12)	0.96 (0.54–1.25)	1.05 (0.83–1.12)
	Met- to Peraluminous	Metaluminous	Met- to Peraluminous	Peraluminous
Fe*	Magnesian < 67.5% SiO_2	Ferroan < 67.5% SiO_2	Magnesian < 67.5% SiO_2	Magnesian -Ferroan > 67.5% SiO_2
Total LREE ppm	279 (11–1329)	497 (83–800)	435 (20–1362)	255 (91–758)
Total REE ppm	316 (52.5–1432)	567 (90–936)	492 (23.5–1497.3)	284 (109.2–861.5)
$(Eu/Eu^*)_N$	0.77 (0.11–10.31)	0.70 (0.31–1.27)	0.61 (0.18–1.42)	0.45 (0.26–0.91)
REE $(La/Yb)_N$	27.5 (0.27–122.37)	12.18 (3.33–54.65)	25.1 (0.95–93.85)	18.52 (3.37–54.03)
LREE $(La/Sm)_N$	4.78 (1.00–14.7)	3.20 (1.24–7.70)	5.93 (2.0– 23.60)	4.71 (2.95–6.11)
HREE $(Gd/Yb)_N$	2.67 (0.23–11.39)	2.26 (1.56–5.11)	2.18 (0.38–6.37)	1.79 (0.65–3.87)
Average T_{Zr} ± σ°C (n_{tot} = 456 samples)	768 ± 51 °C (297)	833 ± 47 °C (43)	788 ± 66 °C (93)	741 ± 48 °C (23)
[εNd(t) full range] (mean)	[1.14, −3.65] (−0.21)	[−0.36, −3.36] (−1.49)	[4.32, −6.43] (−1.66)	[2.79, −8.43] (−5.34)

granitic magma. One concordant analysis at ca. 930 Ma may reflect crystallisation of the granitic magma. The ages are consistent with known ages in the region, and show that unlike the SMB and HBG granites, the Flå granite contains abundant inherited zircon.

4.2. Major and trace element geochemistry

Whole-rock major and trace element data from the Sveconorwegian granitoids are summarised in Table 2. All geochemical major and trace element data are given in Electronic Supplement 2. The rocks are generally undeformed with well-preserved magmatic textures and primary mineralogy, suggesting that very little subsolidus element mobility has taken place and that the geochemical composition of the granitoids reflects their primary magmatic composition. However, like for most intrusive rocks, it is likely that the composition of the granitoids does not represent the true melt composition, but it is rather a mix of melt and cumulates (e.g. Barnes et al., 2016, Deering and Bachmann, 2010). This is likely to be particularly true of the SMB granites, which locally preserves evidence of melt-escape textures from parts of the rocks that are particularly rich in alkali feldspar phenocrysts.

The SMB and HBGout suites mainly range in SiO_2 from 65 to 75 wt %, the HBGin between 65 and 70 wt% and the FIB suite between 70 and 75 wt% SiO_2. In the Fe* versus SiO_2 diagram (Frost et al., 2001), the SMB and HBGout plot as magnesian for SiO_2 < 70 wt%, and straddle the magnesian/ferroan line at higher values (Fig. 4). The HBGin plots as ferroan and the FIB suite, with its high SiO_2, straddles the Fe* line. All four suites show a negative correlation between the major oxides and SiO_2 in the Harker diagrams (Fig. 3), except for K_2O and Na_2O. The K_2O content of the SMB and HBG suites is positively correlated with SiO_2 and is equivalent to high-K and shoshonites, at least in part an effect of alkali feldspar accumulation. Na_2O is uncorrelated, except for a slight decrease at high SiO_2 in the SMB suite. In the A/CNK diagram, the SMB and HBGout suites straddle the boundary between metaluminous and peraluminous compositions, the HBGin suite is distinctly metaluminous, and the FIB suite is distinctly peraluminous (Fig. 5).

All four suites display negatively sloping chondrite-normalised REE patterns, generally with negative Eu anomalies. Although there is complete overlap in REE contents between the SMB and both HBG suites, the HBGin suite is generally higher in REE, has a shallower LREE/HREE (light and heavy REE, respectively) slope, and smaller negative Eu anomalies, than the SMB and HBGout suites (Table 2 and Fig. 6). LREE is similar in the two HBG suites. The FIB has a similar LREE pattern to the SMB and HBGout suites, but with a nearly flat MREE/HREE pattern. Overall, samples with larger negative Eu anomalies have higher total REE concentrations. Also, the Eu anomaly is negatively correlated with SiO_2 content, suggesting that variations in REE concentrations and patterns are largely related to fractionation and/or accumulation of feldspar. In the primitive mantle-normalised diagram, the four suites display positive Rb, K and Pb anomalies and negative Sr, P and Ti anomalies. Pb and K are distinctly positive and show very little scatter. All the suites show negative, but variable Nb-Ta anomalies, ranging from moderate in the HBGin suite to more strongly negative in the other suites. Unlike the SMB and HBG suites, the FIB suite displays significant U-Th enrichment (defined as high heat-producing granites by Slagstad (2008)). The HBGin suite exhibits mainly positive Ba anomalies and SMB and HBGout suites show variable negative and positive Ba anomalies, whereas the FIB suite only has negative Ba anomalies. The distinctly ferroan HBGin is the only suite that plots both in the A-type field of Whalen et al. (1987) and as a within-plate granite (WPG) of Pearce et al. (1984).

4.3. Zircon trace element concentrations

Zircon trace element data from SMB and HBGs, presented in Electronic Supplement 3, provide a nearly continuous record of magmatism from ca. 1070 to 920 Ma and show relatively little variation. All samples are characterised by positively sloping REE patterns with relatively strong positive Ce anomalies and moderately negative Eu anomalies (Fig. 7A). Relative LREE enrichment may be related to gain of non-formula elements during hydrothermal activity (Hoskin, 2005, Rayner et al., 2005). Fig. 7B shows a plot of Nb/Yb versus Gd/Yb trace element compositions. The diagram is designed to reveal the stability of garnet in the source, which would retain the heavy REEs (represented by Yb) in the residue and result in a positive trend towards higher Nb/Yb and Gd/Yb ratios (Grimes et al., 2015). No such trend is observed in the available dataset.

4.4. Zircon saturation temperatures

Temperatures for the SMB, HBGin, HBGout and FIB suites (Fig. 8) have been estimated using the zircon saturation temperature (T_{Zr}) geochemical thermometer based on the works by Watson and Harrison (1983) and the revised model and equation by Boehnke et al. (2013). Only samples with M cation ratios ($M = (Na + K + 2{\cdot}Ca)/(Al{\cdot}Si)$) within the calibration range (M = 0.9–1.9) were selected for T_{Zr} calculation and the assumed stoichiometric zirconium content for zircon is 497,646 ppm, based on Hanchar and Watson (2003). The results of the temperature calculations are given as the suite average ± one standard

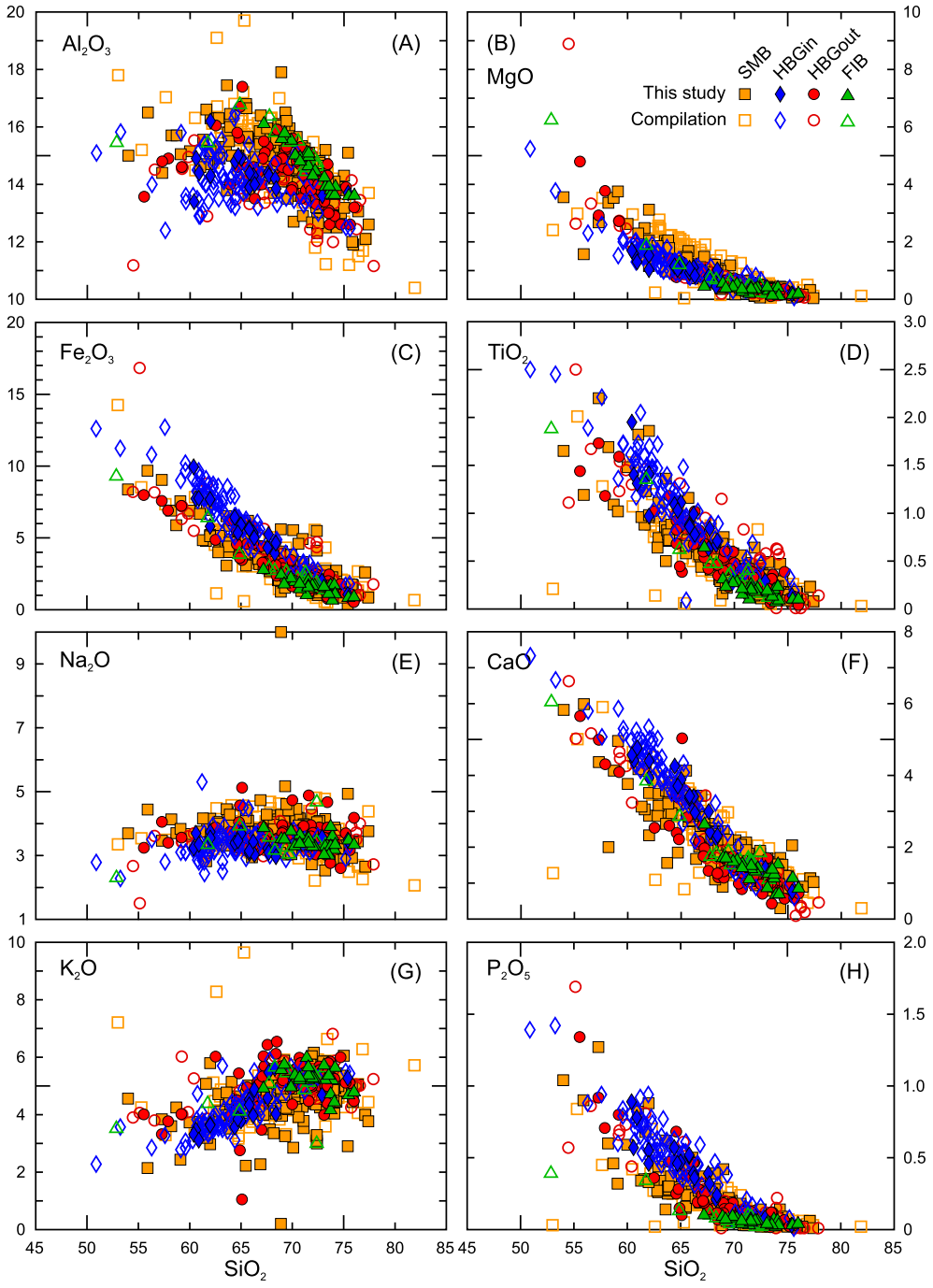

Fig. 3. Major element variation in granitoid suites of the Sveconorwegian Province, given in wt. %. (A) Al_2O_3. (B) MgO. (C) Fe_2O_3. (D) TiO_2. (E) Na_2O. (F) CaO. (G) K_2O. (H) P_2O_5. Filled symbols are new data from this study, while non-filled symbols are the compiled data (Table 1).

deviation. Zircon saturation temperatures and M values for each sample are presented in Electronic Supplement 2.

The mean T_{Zr} for the SMB is 768 ± 51 °C, while the ferroan HBGin shows on average higher T_{Zr} at 833 ± 47 °C. The HBGout suite yields 788 ± 66 °C, similar to the SMB suite, while the FIB suite shows the overall lowest T_{Zr} with an average of 741 ± 48 °C. The calculation depends solely only on the whole-rock composition and is given by the compositional parameter M and the Zr bulk content, which raises several uncertainties. The method has the underlying assumptions that the whole-rock composition is as close as or equal to melt composition and that all zircons have crystallised from the melt. Firstly, granitoids rarely reflect melt compositions but is rather a product of magmatic differentiation. Differentiation leads to a decrease of the compositional parameter M (increase of SiO_2 content) and increase of Zr content (Harrison et al., 2007), which results in temperature variations that can be in the order of hundreds of degrees when compared to conditions prior to differentiation (Siégel et al., 2018). Also, the data set have examples in all four suites that some of the estimated temperatures fall below ~700 °C, which is below solidus for most granites. Secondly, the presence of inherited zircons in the magma would result in Zr contents that are too high for the given magma composition (Miller et al., 2003), as the Zr content is the sum of the Zr saturated in the magma but also the Zr residing in the inherited zircons. We know from other lines of evidence that the FIB suite contains a significant number of inherited zircons, therefore yielding overestimated temperatures and can therefore only be regarded as maximum temperatures (Miller et al., 2003). In

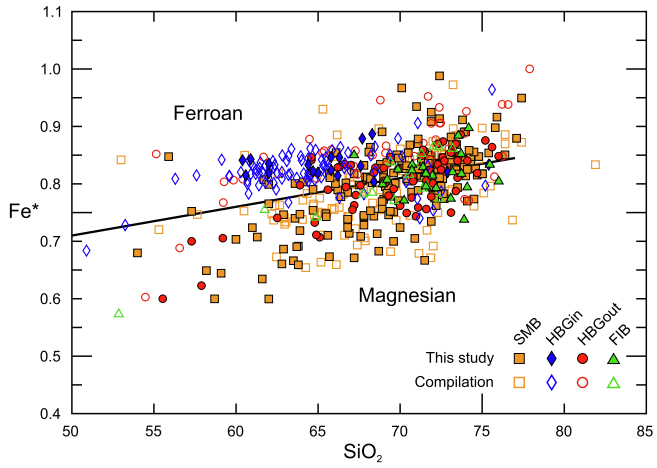

Fig. 4. Fe* versus SiO_2 (wt. %) discrimination diagram after Frost et al. (2001). Fe* = $FeO_{tot}/(FeO_{tot} + MgO)$.

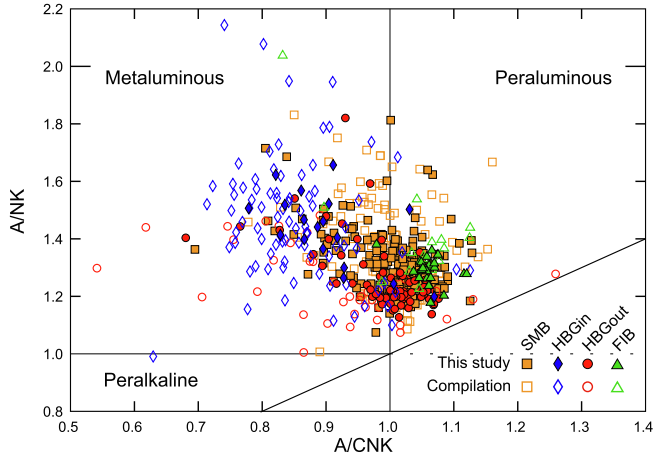

Fig. 5. A/NK versus A/CNK plot showing the levels of alumina saturation of the four granitoid suites of the Sveconorwegian Province. A/NK and A/CNK is calculated by dividing each oxide on its molecular weight.

contrast, The SMB and HBG suites do not contain inherited zircons, suggesting that the estimated zircon saturation temperatures are valid and can be regarded as minimum temperatures according to Miller et al. (2003). Regardless of the choice of model (Boehnke et al., 2013, Watson and Harrison, 1983), the predicted saturation temperatures for the four magmatic suites reveal the same trend, with increasing temperatures associated with the transition from the SMB to the HBG suites, where the HBGin suite shows the highest overall temperatures.

4.5. Sm-Nd isotopic data

The whole-rock Sm-Nd isotopic data presented here comprise new data and compiled data from the literature (Fig. 9A and B) and are listed in Table 1. The Sm-Nd isotopic data and corresponding ages can be found in the Electronic Supplement 4. All εNd(t) values are calculated based on crystallisation ages from its original reference or obtained by later dating of the same intrusion. Undated HBGin and HBGout intrusions have been assigned an age of 950 Ma, which is the suggested age of peak HBG magmatic activity (Slagstad et al., 2018b). An average age of 1040 Ma is inferred for the SMB suite, based on Bingen et al. (1993). The εNd(t) values for the SMB suite range from +1 to −2. The HBGin and HBGout are indistinguishable based on their isotopic composition with εNd(t) values generally from 0 to −5. When the HBG suites are back-calculated to SMB ages at 1040 Ma, they display a total overlap with the SMB suite, and both suites plot on the evolutionary trend from the local ca. 1.5 Ga basement. Three ~1.2 Ga samples plot in the lower half of the ~1.2 Ga-field (Fig. 9A), overlapping with the evolutionary trend from the 1.5 Ga basement. Two of these samples are granitic gneisses from the Setesdalen area and the lowermost symbol is from a granitic gneiss xenolith in the SMB suite. The FIB suite shows the lowest (i.e., most unradiogenic) initial εNd(t) values of the four suites at −3 to lower than −8. The FIB suite overlaps with the evolutionary curve of the TIB granitoid rocks that make up the Eastern Segment and orogenic foreland.

5. Discussion

5.1. Potential lower-crustal sources of the Sveconorwegian magmatism

The western and central Sveconorwegian Province contains evidence of several major magmatic events prior to the Sveconorwegian orogeny. The oldest exposed basement is ca. 1.52–1.48 Ga (Bingen et al., 2005, Roberts et al., 2013) and comprises volcanic and plutonic protoliths variably metamorphosed between upper greenschist and granulite facies (Coint et al., 2015, Menuge and Brewer, 1996, Roberts et al., 2013). Younger granitoid orthogneisses are interpreted to represent a magmatic event at ca. 1.28–1.20 Ga (Pedersen et al., 2009; Slagstad et al., 2018). The 1.5 Ga and 1.25 Ga rocks both show juvenile signatures close to depleted mantle values, however, the 1.25 Ga suite appear to be too juvenile to yield magmas of SMB and HBG composition without the addition of a more unradiogenic source for which there is no direct evidence. The 1.5 Ga rocks show on average εNd(t) values that are consistent with the isotopic signatures of the SMB and HBG suites and appear to be the most likely source for these granitoid suites. Assuming a dominantly lower-crustal, ca. 1.5 Ga source for the Sveconorwegian granitoids, as suggested by the isotopic data, our petrogenetic model involves a first stage of melting and extraction to form the SMB suite, leaving a depleted, dehydrated lower-crustal residue. Second stage, low degree melting of the depleted and dehydrated lower-crustal residue may have formed the HBGin suite. The two-stage setup is based on the geochronological constraints on the SMB and HBG magmatism (e.g. Andersen et al., 2007, Coint et al., 2015, Fig. 9 in Slagstad et al., 2018b). Below, we test this two-stage hypothesis using trace element modelling and discuss the tectonic implications of this model.

5.2. Trace element modelling of the SMB and HBG suites

REE, Ba, Rb, Sr, U, Th, Nb and Ta concentrations in partial melts and the complementary residues were modelled to test the hypothesis outlined above. Partition coefficients compiled from literature and used for the trace element modelling are given in Table 3. The modelling was done in two stages to accommodate changes in starting composition and residual mineral assemblage. Our data suggest that deformation was taking place throughout the period, indicating that a Rayleigh model with instant melt-removal is an appropriate choice of model for both melting stages (Fig. 10). The same partition coefficients for intermediate (dacite-andesite) melt compositions were used for both melting stages (Table 3). The average composition of the 1.5 Ga rocks (Roberts et al., 2013) were the chosen as the starting composition for stage 1 (Table 3).

Model melts for variable degrees of melting during stage 1 were compared with average SMB suite compositions. The SMB suite shows a highly variable abundance of alkali feldspar phenocrysts, ranging from non-existent to constituting > 80 vol% of the rock (Coint et al., 2015). As discussed above, this variable accumulation of alkali feldspar probably has a major impact on the trace element composition of the SMB suite and would produce pronounced positive Eu anomalies and decreased overall REE concentrations. To alleviate the effects of alkali feldspar accumulation and to approximate the primary melt composition of the SMB suite, an average SMB suite composition was calculated from samples with Eu anomalies < 0.9 (which corresponds to ~80% of

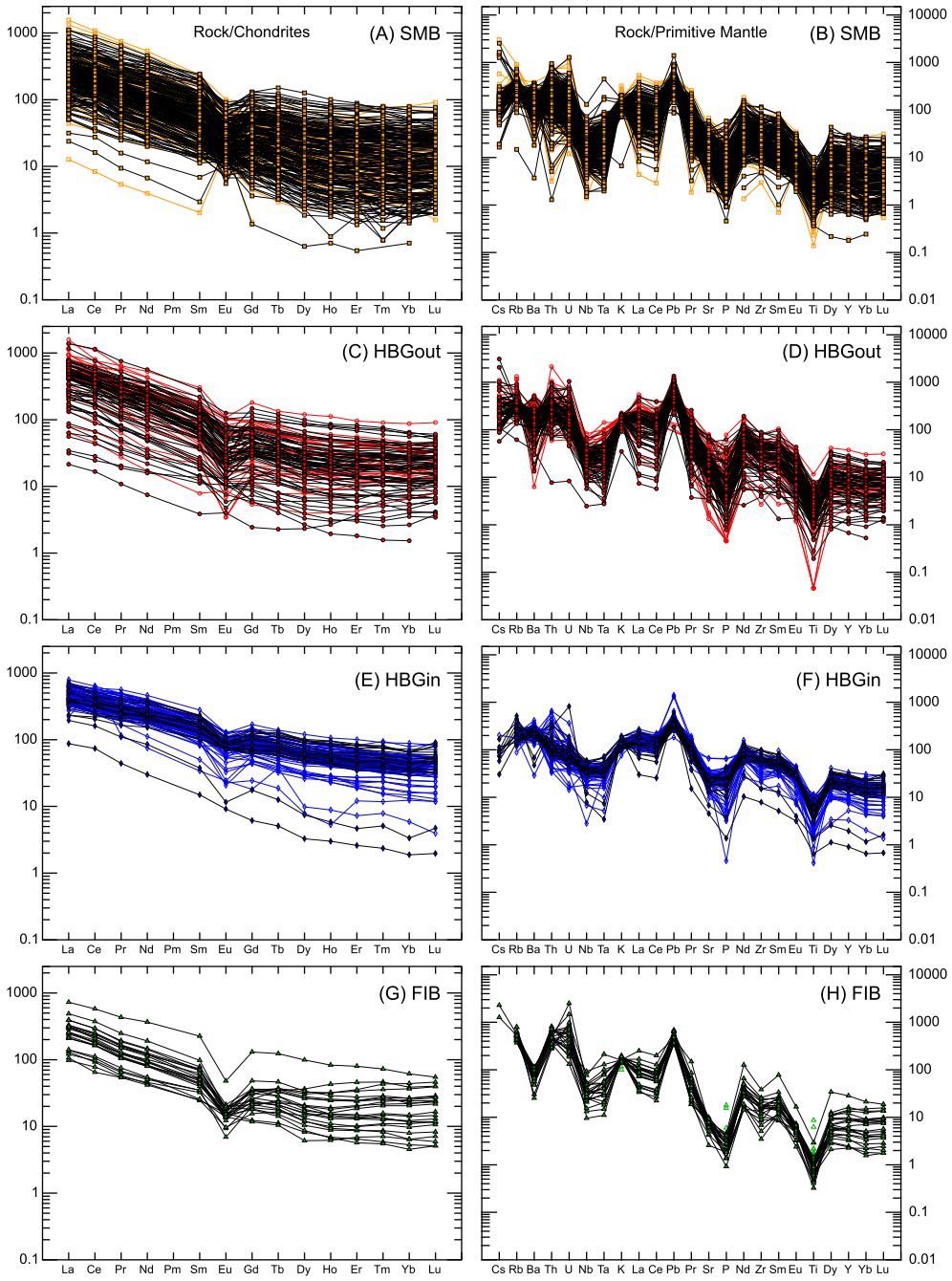

Fig. 6. Chondrite-normalised REE and primitive mantle-normalised trace element patterns for the four granitoid suites. Chondrite and primitive mantle values are from Sun and McDonough (1989). Filled symbols with black lines are new data from this study, whereas non-filled symbols with coloured lines are the compiled data (Table 1). Single points in spider diagram for FIB (inset H) are due to the lack of several REEs.

total SMB data), as feldspar cumulates tend to produce positive anomalies (Eu anomalies > 1). For stage 2, model melts were compared with the average composition of the HBGin suite.

5.2.1. Stage 1: partial melting of the lower crust and SMB suite formation

Trace element concentrations were calculated for melt fractions (F) of 10, 20 and 50%. Results show that 50% partial melting of a 1.5 Ga source yields trace element compositions that are similar to the SMB with characteristic negative Sr, Nb-Ta and Eu anomalies, whereas lower melt fractions (10 and 20%), produces melts, enriched in incompatible trace elements well above the levels observed in the SMB (Fig. 10A). Hence the model with 50% melting is most likely from the trace element data, leaving a residue comprising plagioclase (20%), orthopyroxene (45%), clinopyroxene (30%) and minor amphibole (5%). The 1.5 Ga orthogneisses have been interpreted to represent mature arc rocks and comprise metavolcanic and -plutonic rocks ranging in composition from gabbro, diorite, granodiorite, granite to tonalite (Roberts et al., 2013). They have a typical arc-like signature with negative Nb–Ta and Ti anomalies and juvenile isotopic compositions, with εNd(t) values ranging from +1 to +5 (Fig. 9A), suggesting that the geochemical features of the 1.5 Ga rocks reflect subduction-zone processes. The trace element modelling shows that a partial melt is likely to inherit these features. Thus, using these geochemical anomalies as the single discriminant for an arc setting is misleading.

We used a simple binary mixing calculation to investigate the proportion of crustal component that can be mixed with depleted mantle

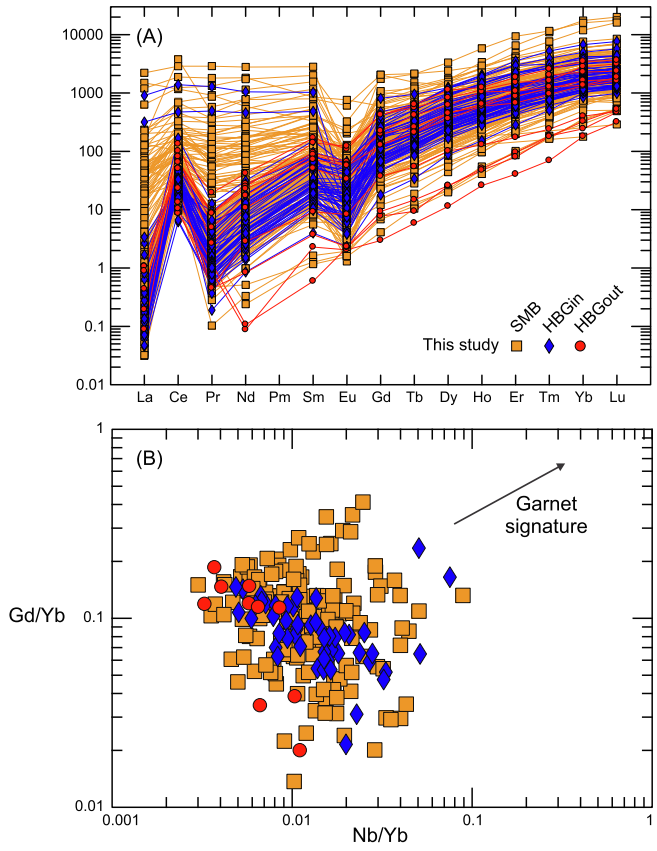

Fig. 7. Zircon trace elements. A) Chondrite-normalised REE patterns of zircons. Normalisation values after Sun and McDonough (1989). B) Gd/Yb versus Nb/Yb diagram after Grimes et al. (2015).

before the mantle contribution is indistinguishable in the isotopic composition of SMB suite (Fig. 9B). The juvenile end-member was based on DePaolo (1981)'s depleted mantle model and approximated value for 1040 Ma with initial $^{143}Nd/^{144}Nd = 0.5115855$ and Nd = 6.22 ppm (primitive lava composition from Whattam (2018)). The average isotopic composition of the 1.5 Ga rocks recalculated to 1040 Ma was chosen to represent the crustal end-member with initial $^{143}Nd/^{144}Nd = 0.511301897$ and Nd = 66 ppm (from trace element modelling of Nd at 50% partial melting). Our calculations indicate that small amounts of crustal component will significantly modify the isotopic composition towards a more crustal composition and that a composite melt consisting of 30 wt% crustally derived melt mixed with 70 wt% depleted mantle melt cannot be distinguished from a pure crustal melt.

5.2.2. Stage 2: partial melting of a residual source and HBGin suite formation

The residue after 50% partial melting in stage 1 was used as the starting composition for stage 2 melting. Trace element concentrations were calculated for melt fractions of 5, 10 and 20%, leaving behind a dehydrated residue consisting of plagioclase (15%), orthopyroxene (65%) and clinopyroxene (20%). The modelling shows that model melts comparable to the HBGin suite can be produced by small degrees of partial melting (F = 5–10%) (Fig. 10B). At this point, all hydrous phases have been consumed. The lower crust is completely anhydrous and strongly depleted in incompatible elements, uranium and thorium, consistent with the low heat-flow values for the western parts of the Sveconorwegian Province (Slagstad et al., 2009). The trace element modelling suggests that melting a dehydrated and depleted source can produce trace element-enriched melts by low degrees of partial melting.

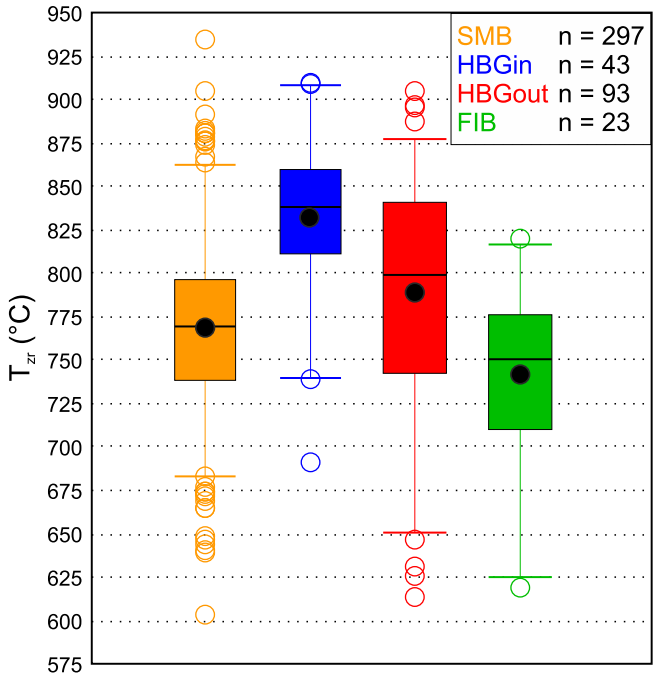

Fig. 8. Temperature estimates of the granitoid suites using zircon saturation temperature (T_{Zr}) thermometer after Watson and Harrison (1983). T_{Zr} is calculated using the revised formula of Boehnke et al. (2013) and is given in Celsius with $T_{Zr} = 10108 / \ln(D_{Zr}) + 1.16 \times (M-1) + 1.48)-273.15$ °C, where D_{Zr} is the distribution coefficient of zirconium between zircon and the melt, given by the stoichiometric amounts of 497,646 ppm Zr in zircon after Hanchar and Watson (2003) divided by Zr (ppm) whole-rock content of each analysed sample. M is ratio between cation fractions between the alkalis and aluminium multiplied with silicon and is calculated by M = (Na + K + 2·Ca)/(Al·Si) (see Hanchar and Watson (2003) for step-by-step calculation). 273.15 is subtracted for converting the temperature from Kelvin to Celsius. All samples plotted are within the compositional calibration range of M = 0.9 – 1.9. The black circle represents the mean of the distribution, black line is the median, the bottom and top of the coloured box is the Q1–Q3 (quartile) range and the whiskers are the 5% and 95% of the data, thus samples in the 5% and 95% are outliers and are plotted as individual samples.

5.3. SMB and HBG petrogenesis

Formation of the SMB suite at 1070–1010 Ma and the HBGin suite at 1000–920 Ma is associated with an increase in the estimated temperature (Table 2) and an overall change in the alumina saturation level (from metaluminous/peraluminous to metaluminous). The HBGin suite can be considered to have an A-type-like composition due to its ferroan nature, enrichment in incompatible elements and it is the only suite that plots both in the A-type field of Whalen et al. (1987) and as a within-plate granite (WPG) of Pearce et al. (1984). Dehydration melting is usually the preferred mode of melting in the lower crust, where the only available water is structurally bound in hydrous minerals such amphibole and biotite (Whitney, 1988). These dehydration-melting reactions have a thermal buffering effect on the system, but once the hydrous phases are consumed the temperature can continue to rise (Landenberger and Collins, 1996). During dehydration melting, hydrous phases such biotite and amphibole break down, releasing the excess Al and other incompatible elements into the melt making it peraluminous while Ca and other compatible components are retained to form pyroxene-rich mineral assemblages. A further increase of the temperature, as indicated by the HBGin suite, suggests that Ca-pyroxenes in the residue started to melt and thus resulted in formation of more metaluminous melts (A/CNK ratios < 1) (e.g. Chappell et al., 2012). Several authors have proposed residual melting as a mechanism to form A-type granites (e.g. Collins et al., 1982, Landenberger and

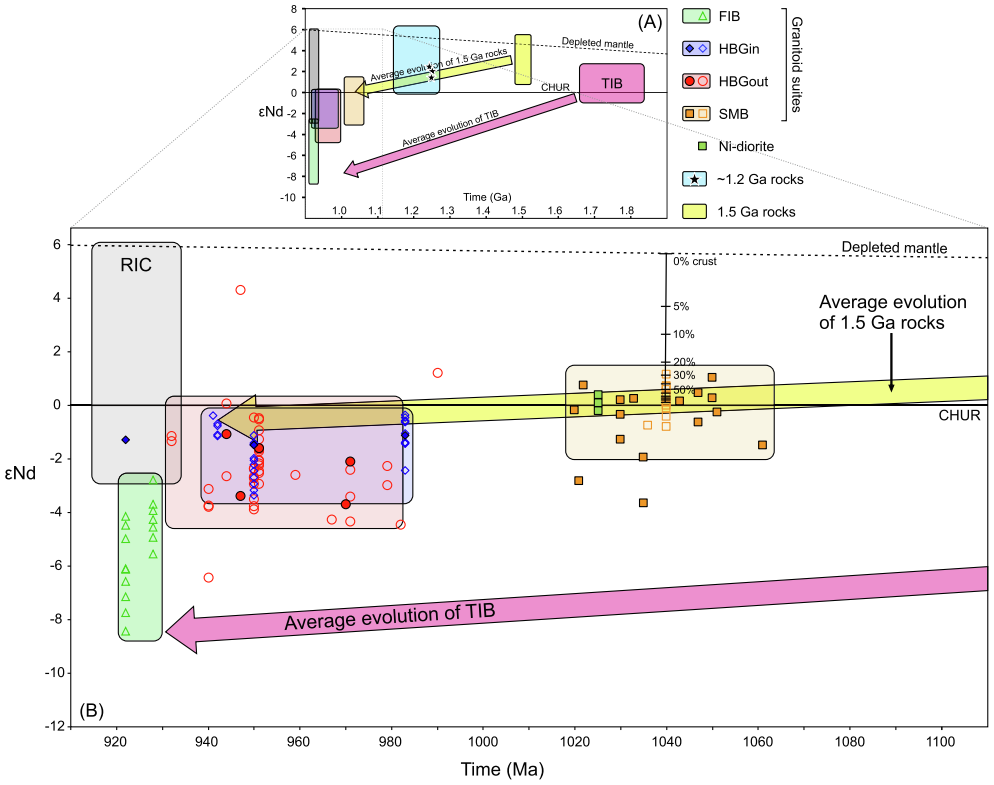

Fig. 9. Whole-rock Nd isotopic ratios from granitoid samples from the Sveconorwegian Province. Plot of εNd(t) versus time, where t = crystallisation age of associated granitoid sample. Filled symbols are new data from this study, whereas non-filled symbols are the compiled data (Table 1). εNd(t) values were calculated relative to CHUR with present day values: $\varepsilon Nd(t) = [([(^{143}Nd/^{144}Nd)_{rock} - (^{147}Sm/^{144}Nd)_{rock} \times (\exp^{\lambda t}-1)]/[(^{143}Nd/^{144}Nd)_{CHUR} - (^{147}Sm/^{144}Nd)_{CHUR} \times (\exp^{\lambda t}-1)])-1] \times 10.000$, with present-day CHUR values of $^{143}Nd/^{144}Nd_{CHUR} = 0.512638$ (Goldstein et al., 1984) and $^{147}Sm/^{144}Nd_{CHUR} = 0.1967$ (Jacobsen and Wasserburg, 1980) and Sm-Nd decay constant of $\lambda = 6.54 \times 10^{-12}$ (Lugmair and Marti, 1978). Depleted mantle evolution is according to DePaolo (1981), which is $\varepsilon Nd(t) = 0.25t^2 - 3t + 8.5$ and where t is age. (A) Inset displaying the isotopic evolution between 1.9 and 0.9 Ga. (B) Detailed view of the isotopic evolution between 1100 and 900 Ma. SMB – Sirdal Magmatic Belt; HBGin – HBG inside SMB; HBGout – HBG outside SMB; FIB – Flå-Iddefjord-Bohus; TIB – Transscandinavian Intrusive Belt; RIC – Rogaland Igneous Complex. Undated HBGin and HBGout intrusions have been assigned an age of 950 Ma, which is the suggested age of peak HBG magmatic activity (Slagstad et al., 2018b). An age of 1040 Ma is inferred for the undated SMB suite samples, based on Bingen et al. (1993). Data from the granitoid suites and samples with their corresponding ages used for calculation εNd(t) can be found in Electronic Supplement 4. Sources: The Nd isotopic data from TIB and RIC rocks is from Bingen et al. (2011)'s isotopic compilation. The isotopic data for the ~1.25 and 1.5 Ga rocks outlined in inset (A) is from Brewer and Menuge (1998), Brewer et al. (2002) and Brewer et al. (2004).

Table 3
Partition coefficients and natural compositions used in two-stage modelling of partial melting of the lower crust and stage 1 residue. Mean composition of the 1.5 Ga rocks were used as the starting composition for stage 1 melting. Mean SMB (with Eu anomalies < 0.9) and HBGin natural compositions used for comparing stage 1 and 2 melting products. Compositions are given in ppm.

	Partition coefficients				Model compositions		
	Pl	Hbl	Cpx	Opx	1.5 Ga	SMB	HBGin
Rb	0.2[6]	0.14[5]	0.1[6]	0.0038[1]	122.64	198.4	125.14
Ba	0.21[14]	0.12[5]	0.1[15]	0.0036[1]	639.85	983.8	1632.96
Th	0.04[14]	0.5[6]	0.1[3]	0.0005[1]	10.02	23.4	11.53
U	0.01[6]	0.1[6]	0.04[6]	0.0007[1]	2.92	4.0	1.88
Nb	0.0265[8*]	0.2[5]	0.22[1]	0.0007[1]	8.97	14.5	24.61
Ta	0.0595[7*]	0.21[5]	0.43[3]	0.0008[1]	0.55	1.1	1.46
Sr	2.41[14]	0.28[5]	0.07[6]	0.0019[1]	243.13	344.4	505.14
La	0.3926[9]	0.435[11]	0.1[11]	0.016[4]	36.49	76.0	105.64
Ce	0.2511[9]	0.545[11]	0.2[11]	0.019[4]	75.10	151.3	226.89
Nd	0.189[9]	0.33[2]	0.31[2]	0.03[4]	36.95	64.3	118.04
Sm	0.1366[9]	1.46[11]	0.6[11]	0.042[4]	7.66	11.6	21.91
Eu	2.11[16]	1.49[11]	0.6[11]	0.052[4]	1.47	1.7	4.59
Gd	0.1202[13]	1.72[11]	0.7[15]	0.034[10]	6.29	8.1	18.40
Tb	0[9]	1.96[11]	0.7[11]	0.08[4]	1.13	1.3	2.74
Yb	0.1323[9]	1.42[11]	0.6[11]	0.36[4]	3.58	3.2	7.09
Lu	0.1384[9]	1.31[11]	0.6[11]	0.45[4]	0.55	0.5	1.03

Partition coefficients references: (1) Adam and Green (2006); (2) Arth and Hanson (1975); (3) Bacon and Druitt (1988); (4) Borg and Clynne (1998); (5) Brenan et al. (1995); (6) Dostal et al. (1983); (7) Dudas et al. (1971); (8) Dunn and Sen (1994); (9) Fujimaki et al. (1984); (10) Green et al. (2000); (11) Martin (1987); (12) Matsui et al. (1977); (13) Nagasawa and Schnetzler (1971); (14) Okamoto (1979); (15) Reid (1983); (16) Schnetzler and Philpotts (1970). *Estimated value.

Collins, 1996). Collins et al. (1982) suggested that the A-type granites in the Lachlan Fold Belt were formed by vapor-absent melting of a dehydrated and depleted granulitic source in the lower crust, whereas Landenberger and Collins (1996) proposed a similar model for the A-type granites in the Chaelundi Complex in eastern Australia, by melting of a dehydrated but not melt-depleted residual source. Both of these studies point out that these A-type granites were generated and emplaced after the I-type granites, indicating the source they were derived from have been affected by earlier dehydration and melting processes. Also, both studies indicated elevated temperatures in excess of 900 °C (Landenberger and Collins, 1996) or at least higher than the first melt extraction event (Collins et al., 1982) was crucial to induce melting to form A-type granites. The temporal and spatial relationship of the SMB and HBGin suite indicate that the HBGin suite is derived from a source region that previously has experienced melt extraction and when the source region is melting for the second time, it is dehydrated and depleted. The trace element modelling suggests that melting a dehydrated and depleted source can produce trace element-enriched melts by low degrees of partial melting. Low degrees of partial melting will produce REE-enriched melts with high LREE/HREE ratios, as the LREEs are more compatible into melt than the HREEs. The ratios ($(La/Lu)_N$ ratios in Table 2) of the HBGin suite is lower compared to the other suites but the suite display an overall high REE content. We attribute the lower LREE/HREE ratio directly to the HBGin source, suggesting that it was depleted at the time of melting and had already lost LREE-enriched melt at a previous stage. Melting experiments show that significant amounts of melting can take place within the same temperature intervals for hydrous and anhydrous mineral assemblages (e.g. Beard et al., 1994, Clemens et al., 1986, Clemens and Vielzeuf, 1987), suggesting that it is plausible to melt an anhydrous mineral assemblage with a continuous heat supply. This shows that the composition of the extracted melts will change over time as the composition of the lower crust changes.

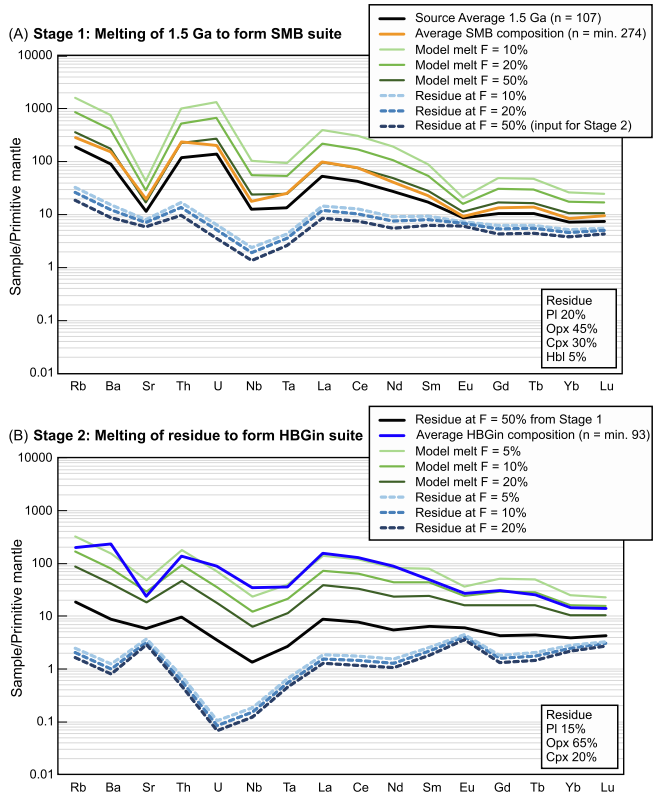

Fig. 10. Trace element modelling results from two-stage Rayleigh partial melting. (A) Stage 1: Model melt obtained by 50% partial melting of the 1.5 Ga rocks of Roberts et al. (2013) is similar to the SMB suite composition in trace element enrichment. (B) Stage 2: 5 – 10% partial melting of lower crustal residue following 50% partial melting in stage 1 produce melt that is comparable to HBGin compositions. Both stages are dominated by plagioclase, orthopyroxene and clinopyroxene, with minor hornblende in stage 1. A change in melt fraction have a major effect on the trace element levels of the melt but have little effect on the slope of the model curve. Chosen partition coefficients are appropriate for intermediate compositions and is listed in Table 3. Residual phases are given in weight proportions. Pl – plagioclase; Opx – orthopyroxene; Cpx – clinopyroxene; Hbl – hornblende.

The geochemical and isotopic compositions of the SMB and HBGout suites are indistinguishable; the HBGout suite exhibits the same spread in trace element concentration, similar alumina-saturation level (A/CNK) and iron enrichment (Fe*) as the SMB suite, and the HBGout suite plots on the same εNd(t) evolutionary path as the SMB suite. The compositional similarities of the SMB and HBGout suites suggest that these suites formed from a similar source through similar lower-crustal processes at similar temperatures. The HBGout suite is thus interpreted to represent first-stage melting of the lower crust in the same manner as the SMB, just farther east. The geographically widespread lower-crustal melting coincided with a transition from a generally compressional setting prior to ca. 1000 Ma, to a generally extensional setting after. This shows that not only did the lower-crustal sources change over time, with remelting of dehydrated and depleted lower crust, but that new sources and areas became active as the orogen evolved. The trace element composition of zircons from the SMB, HBGin and HBGout suggest that garnet was not a stable phase, indicating that the western and central Sveconorwegian crust never attained a considerable large thickness (Fig. 7B). Although the PT conditions of garnet stability will vary depending on composition, several studies suggest a threshold around 10 kbar (~35 km), below which garnet is unstable (e.g. Garrido et al., 2006, Jagoutz and Schmidt, 2013). This result is also consistent with data from the Rogaland Anorthosite Complex, in the orogenic 'hinterland', that constrain the Moho depth to ca. 35 km at ca. 1040 Ma (Bybee et al., 2014). The lack of high-pressure metamorphism in the central and western part of the Province also indicates little or only modest crustal thickening.

5.4. Flå-Iddefjord-Bohus suite petrogenesis

The FIB suite is situated in the Idefjorden lithotectonic unit in the eastern part of the Sveconorwegian Province. The FIB suite is distinctly high in SiO_2, lacks more mafic end-members and is dominantly peraluminous with A/CNK > 1. The major mafic mineral in the Bohus pluton is biotite with local magmatic muscovite and garnet, which is consistent with its peraluminous character (Eliasson, 1992, Eliasson et al., 2003). However, P_2O_5 content is low in the FIB suite, which stands in contrast to granites that are derived from metasedimentary sources that are strongly peraluminous and high in P_2O_5 (Chappell, 1999). Generally, more mafic granitoids that are derived from melting of metasediments are usually more peraluminous than its more felsic counterparts (e.g. Chappell and White, 1992), whereas the more mafic samples from the FIB suite are metaluminous (Fig. 5). Further, the radioactive element concentration (U, Th and K) of the suite is relatively high compared to average values of granites (Killeen and Heier, 1975b, Killeen and Heier, 1975a, Slagstad, 2008). However, Eliasson (1992) pointed out that samples with high $\delta^{18}O$ whole-rock values were associated with more aluminous two-mica granites, suggesting that a portion of the Bohus is also contaminated by the metasedimentary material, possibly by the directly overlying supracrustal gneisses of the Store Le-Marstrand formation, as later documented by Eliasson et al. (2003). This suggests that at least some of the source material for the Bohus pluton is locally derived from the Idefjorden lithotectonic unit.

Binary mixing modelling between a depleted mantle end-member and a more evolved end-member shows that even small amounts of crustal input will significantly alter the isotopic signature of the melt towards more evolved compositions. Consequently, in cases where the crustal end-member are more evolved (more negative εNd(t) values) less crustal input is needed to drastically shift the isotopic composition of a mantle-derived magma towards more evolved compositions. Even if the FIB suite was mantle-derived or a result of mixing with a crustal source, we would expect to observe a compositional range from mafic to felsic within the magmatic suite. Instead, all the samples are granitic. Furthermore, the presence of abundant inherited zircons in the FIB suite with a range of older zircon core ages for the Flå granite (Fig. 2C) indicate that a significant crustal component was involved in the generation of the FIB melts. The latter is also consistent with the low temperature of crystallization (650–600 °C) estimated by Eliasson and Schöberg (1991) based on zircon saturation temperatures and the lower Zr saturation temperature calculated (741 ± 48 °C) in this study.

The isotopic data from the FIB suite show rather evolved εNd(t) values ranging from −4 to −8, suggesting that it was derived from older continental crust with significant longer residence time, which stands in strong contrast to the isotopic features of the SMB, HBGin and HBGout suites. The age difference between the formation of the TIB lithologies and the FIB suite gave TIB time to develop radiogenic isotopic compositions with very negative εNd values. This suggest that TIB was reworked during the Sveconorwegian orogeny and is a likely contributor to the FIB melts.

5.5. Petrogenetic model and tectonic implications

The proposed model (Fig. 11) for the SMB involves ponding of mafic magma and lower crustal melting resulting in voluminous granitic and minor mafic magmatism from 1070 to 1010 Ma, essentially along the lines suggested by Slagstad et al., 2018b, who also proposed that this mafic magmatism was the main driver for high- to ultrahigh-temperature metamorphism in the southwestern part of the Province. Following SMB magmatism, there is an apparent increase in temperature and geographical extent associated with the transition to HBGin and

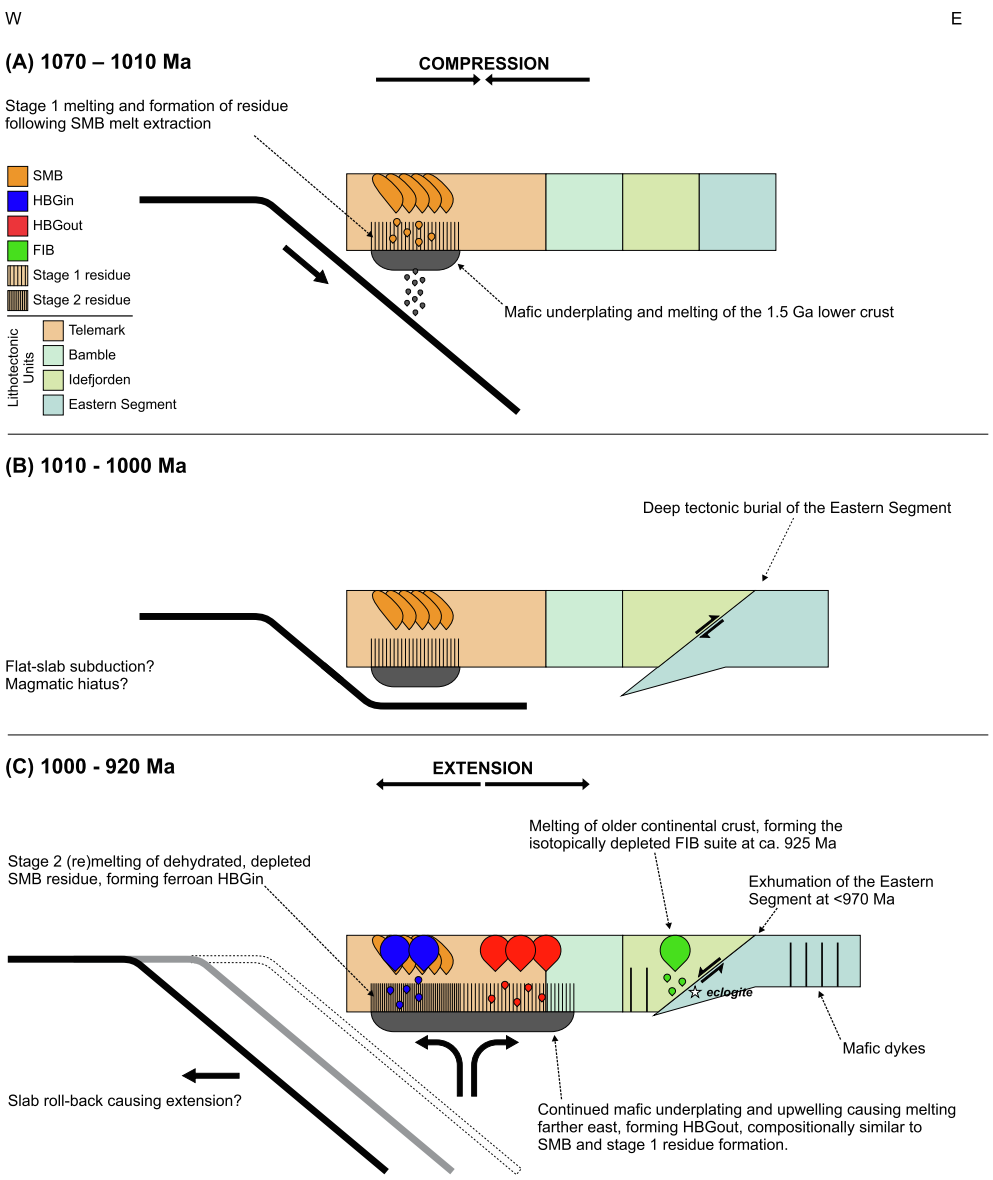

Fig. 11. A schematic tectonomagmatic model for the generation and emplacement of magmatic rocks in the Sveconorwegian Province. (A) 1070–1010 Ma: Mafic underplating causes partial melting of the 1.5 Ga lower crustal source leading to formation of SMB melts. The SMB melt extraction leaves behind a dehydrated and depleted lower crustal residue. (B) 1010–1000 Ma: Continued subduction and overall compression leads to deep subduction of the Eastern Segment in the eastern part of the Province, leading to overriding and flattening of the subducting slab and shifting of the magmatism characteristics. (B) 1000–920 Ma: Slab roll back causes extension across the Province initiating widespread mafic underplating and asthenospheric upwelling, which melts the SMB residue at higher temperature to produce the ferroan HBGin suite and the HBGout suite at lower temperature further east. Melting of the older TIB crust gives rise to the FIB suite that is emplaced in the Idefjorden lithotectonic unit.

HBGout magmatism. The rise in temperature associated with the transition from SMB to HBG magmatism at ca. 1000–990 Ma indicates input of additional heat into the lower crust, a reduction in thermal buffering from crustal melting or a combination of the two. The trace element modelling suggests that the HBGin may have formed by partial melting of the dry, chemically depleted lower-crustal residue after SMB extraction. This more refractory lower crust would have allowed temperatures to rise even more before consuming heat by melting and does not in itself necessitate a change in tectonic regime. However, emplacement of the HBGout suggests more widespread lower-crustal melting after ca. 1000 Ma, involving sources that had remained inactive earlier in the orogenic history. We know from several lines of evidence that there was a shift in the regional stress regime from compressional to extensional around 1000 Ma, including emplacement of the Blekinge-Dalarna dolerites in the eastern parts of the Province between ca. 980 and 945 Ma (Söderlund et al., 2005) and E-W directed crustal extension accommodated by the Mylonite Zone (Viola et al., 2011) leading to exhumation of eclogites (Möller et al., 2015). Such an extensional tectonic regime could have allowed more widespread mafic underplating (e.g. Hansen et al., 2015).

Mafic magmatism is scarce relative to the far more abundant felsic magmatism, but it is geographically widespread and emplaced over a long period of time, overlapping with the SMB and HBG suites (Jensen and Corfu, 2016; Slagstad et al., 2018b; Vander Auwera et al., 2011; Wiest et al., 2018). We interpret the disproportions between the felsic and mafic magmatism to reflect ductility and density contrasts between the lower crust and the underplated mafic magmas that prevented further ascent of the denser, mafic magmas (e.g. McLelland et al., 2013). As mafic magmas rise through the crust it is likely to stall in the mid-crust as a result of buoyancy loss due to the lower density of the surrounding crustal rocks (e.g. Glazner and Ussler III, 1988). The duration of SMB and HBG magmatism (i.e., ca. 150 million years) is direct evidence that prolonged heating and resultant crustal melting took place in the western and central parts of the Province. Our results also show that although there are chemical variations over time, these variations can be ascribed to depletion of lower-crustal melt sources during evolving orogenesis, rather than a distinct change in tectonic and petrogenetic processes. These observations place some constraints on potential heat sources, i.e. crustal thickening followed by radiogenic self-heating versus mafic underplating. The lack of major compressional structures and absence of high-pressure metamorphism in the western and central parts of the Province suggest that crustal thickening is not a viable heating mechanism leading to the formation of the SMB and HBG suites. In addition, it is difficult to see how this thick, hot crust could be

sustained for such a long period of time without undergoing gravity-driven extension and thinning, in turn resulting in cooling. We therefore argue that the SMB and HBG suites in the western and central parts of the Province formed as a result of long-lived mafic underplating driving lower-crustal melting, with depletion of crustal reservoirs and activation of new reservoirs over time as the orogen evolved; in particular, a change from overall compression between > 1070 and 1010 Ma to overall extension between 990 and 920 Ma appears to have been important.

In contrast, the FIB suite is spatially related to continental subduction in the easternmost parts of the Province. Temporally, however, emplacement of the FIB suite trailed high-pressure metamorphism by several tens of million years, thus the genetic relationship between continental subduction and magmatism is not obvious. Radioactive U, K and Th are by far the most important heat-producing elements in the continental crust. These elements are incompatible during partial melting and concentrated in the upper crust, but with subduction of continental crust, such as the Eastern Segment beneath the Idefjorden lithotectonic unit (Brueckner, 2009), the elements are reintroduced to greater depths where they heat up the surrounding rocks over time (Hacker et al., 2011; Hieronymus and Goes, 2010; Slagstad et al., 2018). Although the time scale of several tens of million years is compatible with such a process, it is not obvious that the amount of heating would be sufficient to lead to partial melting. We know that there was widespread mafic magmatism both east and west of the FIB suite approximately at the same time, so an additional input of mantle-derived heat is not unlikely. The FIB suite does not appear to be genetically related to the other suites but formed as a result of crustal reworking of older sources in the eastern parts of the orogen, compatible with the well-established differences in tectonic regime east and west in the orogen and similar to the model proposed by Brueckner (2009).

6. Conclusion

Compilation of available and new geochemical and isotopic data for the granitoid rocks from the Sveconorwegian Province has enabled the identification of four suites: SMB, HBGin, HBGout and FIB suites. The suites represent 150 million years of magmatism in different parts of the orogen and their characteristics allow us to infer the nature of their sources and genetic relationship, resulting in a regional scale tectono-magmatic model for the Province (Fig. 11).

- The data suggest that long-lived mafic underplating inboard of the active southwestern Fennoscandian margin was the main driving force of the magmatism. Ca. 50% partial melting of 1.5 Ga meta-granitoids, the dominant rock type in the region, appears to be a dominant source of the SMB suite, leaving behind a dehydrated and depleted lower-crustal residue.
- The HBGin suite may have formed by remelting of dehydrated and geochemically depleted SMB residue, whereas the HBGout suite – geochemically equivalent to the formation of the SMB suite – probably formed as a result of melting farther east in the orogen, of a source similar to that of the SMB. The reason for increased temperatures and more widespread melting is probably a change from a dominantly compressional to an extensional tectonic regime.
- In the eastern part of the Province, the FIB suite is genetically unrelated to the other three suites. The suite is derived from melting and reworking of older continental crust (e.g. TIB crust), following westward subduction of the Eastern Segment beneath the Idefjorden lithotectonic unit.
- The main heat source of this long-lived crustal melting appears to be mafic underplating. The interpretation that spatial variation and temporal changes in melt compositions can be ascribed to a continuous tectonic process over 150 Myr appears to rule out crustal thickening as a significant cause of heating.

Declaration of Competing Interest

The authors declare that they have no known competing financial interests or personal relationships that could have appeared to influence the work reported in this paper.

Acknowledgements

We would like to thank Hannes K. Brueckner and an anonymous reviewer for their insightful comments and suggestions improving the manuscript. This study is a part of A. Granseth's PhD project on the granitoid magmatism in the Sveconorwegian Province, funded by the Department of Geoscience and Petroleum, Faculty of Engineering, at the Norwegian University of Science and Technology (NTNU). The Geological Survey of Norway (NGU) is thanked for long-lived, continuous support of the ongoing work in the Sveconorwegian Province. The dated samples were collected as part of NGU project 293400. This is CAMOC contribution nr. 3.

Appendix A. Supplementary data

Supplementary data to this article can be found online at https://doi.org/10.1016/j.precamres.2019.105527.

References

Adam, J., Green, T., 2006. Trace element partitioning between mica-and amphibole-bearing garnet lherzolite and hydrous basanitic melt: 1. Experimental results and the investigation of controls on partitioning behaviour. Contrib. Miner. Petrol. 152, 1–17.
Andersen, T., 1997. Radiogenic isotope systematics of the Herefoss granite, South Norway: an indicator of Sveconorwegian (Grenvillian) crustal evolution in the Baltic Shield. Chem. Geol. 135, 139–158.
Andersen, T., Andersson, U.B., Graham, S., Åberg, G., Simonsen, S.L., 2009a. Granitic magmatism by melting of juvenile continental crust: new constraints on the source of Palaeoproterozoic granitoids in Fennoscandia from Hf isotopes in zircon. J. Geol. Soc. 166, 233–247.
Andersen, T., Andresen, A., Sylvester, A.G., 2001. Nature and distribution of deep crustal reservoirs in the southwestern part of the Baltic Shield: evidence from Nd, Sr and Pb isotope data on late Sveconorwegian granites. J. Geol. Soc. 158, 253–267.
Andersen, T., Andresen, A., Sylvester, A.G., 2002. Timing of late-to post-tectonic Sveconorwegian granitic magmatism in South Norway. Nor. Geol. Unders. 440, 5–18.
Andersen, T., Graham, S., Sylvester, A.G., 2007. Timing and tectonic significance of Sveconorwegian A-type granitic magmatism in Telemark, southern Norway: New results from laser-ablation ICPMS U-Pb dating of zircon. Norges geologiske undersøkelse Bulletin 447, 17–31.
Andersen, T., Graham, S., Sylvester, A.G., 2009b. The geochemistry, Lu–Hf isotope systematics, and petrogenesis of Late Mesoproterozoic A-type granites in southwestern Fennoscandia. Canad. Mineral. 47, 1399–1422.
Andersson, U.B., 1997. Petrogenesis of Some Proterozoic Granitoid Suites and Associated Basic Rocks in Sweden (Geochemistry and Isotope Geology). Uppsala Universitet Doctor of Philosophy.
Arth, J.G., Hanson, G.N., 1975. Geochemistry and origin of the early Precambrian crust of northeastern Minnesota. Geochim. Cosmochim. Acta 39, 325–362.
Bacon, C.R., Druitt, T.H., 1988. Compositional evolution of the zoned calcalkaline magma chamber of Mount Mazama, Crater Lake, Oregon. Contrib. Miner. Petrol. 98, 224–256.
Barnes, C.G., Coint, N., Yoshinobu, A., 2016. Crystal accumulation in a tilted arc batholith. Am. Mineral. 101, 1719–1734.
Beard, J.S., Lofgren, G.E., Sinha, A.K., Tollo, R.P., 1994. Partial melting of apatite-bearing charnockite, granulite, and diorite: Melt compositions, restite mineralogy, and petrologic implications. J. Geophys. Res. Solid Earth 99, 21591–21603.
Bingen, B., 1989. Geochemistry of Sveconorwegian augen gneisses from SW Norway at the amphibolite-granulite facies transition. Nor. Geol. Tidsskr. 69, 177–189.
Bingen, B., Belousova, E.A., Griffin, W.L., 2011. Neoproterozoic recycling of the Sveconorwegian orogenic belt: Detrital-zircon data from the Sparagmite basins in the Scandinavian Caledonides. Precambr. Res. 189, 347–367.
Bingen, B., Corfu, F., Stein, H.J., Whitehouse, M.J., 2015. U-Pb geochronology of the syn-orogenic Knaben molybdenum deposits, Sveconorwegian Orogen, Norway. Geol. Mag. 152, 537–556.
Bingen, B., Demaiffe, D., Hertogen, J., Weis, D., Michot, J., 1993. K-Rich Calc-Alkaline Augen Gneisses of Grenvillian Age in SW Norway: mingling of mantle-derived and crustal components. J. Geol. 101, 763–778.
Bingen, B., Mansfeld, J., Sigmond, E.M., Stein, H., 2002. Baltica-Laurentia link during the Mesoproterozoic: 1.27 Ga development of continental basins in the Sveconorwegian Orogen, southern Norway. Can. J. Earth Sci. 39, 1425–1440.
Bingen, B., Nordgulen, Ø., Viola, G., 2008. A four-phase model for the Sveconorwegian orogeny, SW Scandinavia. Norsk Geologisk Tidsskrift 88, 43.
Bingen, B., Skår, Ø., Marker, M., Sigmond, E.M.O., Nordgulen, Ø., Ragnhildstveit, J.,

Mansfeld, J., Tucker, R.D., Liégeois, J.-P., 2005. Timing of continental building in the Sveconorwegian orogen, SW Scandinavia. Norwegian J. Geol/Norsk Geologisk Forening 85, 87–116.
Bingen, B., van Breemen, O., 1998. Tectonic regimes and terrane boundaries in the high-grade Sveconorwegian belt of SW Norway, inferred from U-Pb zircon geochronology and geochemical signature of augen gneiss suites. J. Geol. Soc. 155, 143–154.
Bingen, B., Viola, G., 2018. The early-Sveconorwegian orogeny in southern Norway: tectonic model involving delamination of the sub-continental lithospheric mantle. Precambr. Res. 313, 170–204.
Blereau, E., Clark, C., Jourdan, F., Johnson, T.E., Taylor, R.J.M., Kinny, P.D., Danišík, M., Hand, M., Eroglu, E., 2019. Closed system behaviour of argon in osumilite records protracted high-T metamorphism within the Rogaland-Vest Agder Sector, Norway. J. Metamorp. Geol.
Boehnke, P., Watson, E.B., Trail, D., Harrison, T.M., Schmitt, A.K., 2013. Zircon saturation re-revisited. Chem. Geol. 351, 324–334.
Bogaerts, M., Scaillet, B., Liégeois, J.-P., Vander Auwera, J., 2003. Petrology and geochemistry of the Lyngdal granodiorite (Southern Norway) and the role of fractional crystallisation in the genesis of Proterozoic ferro-potassic A-type granites. Precambr. Res. 124, 149–184.
Borg, L.E., Clynne, M.A., 1998. The petrogenesis of felsic calc-alkaline magmas from the southernmost Cascades, California: origin by partial melting of basaltic lower crust. J. Petrol. 39, 1197–1222.
Brenan, J., Shaw, H., Ryerson, F., Phinney, D., 1995. Experimental determination of trace-element partitioning between pargasite and a synthetic hydrous andesitic melt. Earth Planet. Sci. Lett. 135, 1–11.
Brewer, T.S., Daly, J.S., Åhäll, K.-I., 1998. Contrasting magmatic arcs in the Palaeoproterozoic of the south-western Baltic Shield. Precambr. Res. 92, 297–315.
Brewer, T.S., Menuge, J.F., 1998. Metamorphic overprinting of Sm-Nd isotopic systems in volcanic rocks: the Telemark supergroup, southern Norway. Chem. Geol. 145, 1–16.
Brewer, T.S., Åhäll, K.-I., Darbyshire, D.P.F., Menuge, J.F., 2002. Geochemistry of late Mesoproterozoic volcanism in southwestern Scandinavia: implications for Sveconorwegian/Grenvillian plate tectonic models. J. Geol. Soc. 159, 129–144.
Brewer, T.S., Åhäll, K.I., Menuge, J.F., Storey, C.D., Parrish, R.R., 2004. Mesoproterozoic bimodal volcanism in SW Norway, evidence for recurring pre-Sveconorwegian continental margin tectonism. Precambr. Res. 134, 249–273.
Brueckner, H.K. 2009. Subduction of continental crust, the origin of post-orogenic granitoids (and anorthosites?) and the evolution of Fennoscandia. 166, 753–762.
Bybee, G.M., Ashwal, L.D., Shirey, S.B., Horan, M., Mock, T., Andersen, T.B., 2014. Pyroxene megacrysts in Proterozoic anorthosites: implications for tectonic setting, magma source and magmatic processes at the Moho. Earth Planet. Sci. Lett. 389, 74–85.
Chappell, B.W., 1999. Aluminium saturation in I- and S-type granites and the characterization of fractionated haplogranites. Lithos 46, 535–551.
Chappell, B.W., Bryant, C.J., Wyborn, D., 2012. Peraluminous I-type granites. Lithos 153, 142–153.
Chappell, B.W., White, A.J.R., 1992. I- and S-type granites in the Lachlan Fold Belt. Earth Environ. Sci. Trans. R. Soc. Edinburgh 83, 1–26.
Clemens, J.D., Holloway, J.R., White, A.J.R., 1986. Origin of an A-type granite: experimental constraints. Am. Mineral. 71, 317–324.
Clemens, J.D., Vielzeuf, D., 1987. Constraints on melting and magma production in the crust. Earth Planet. Sci. Lett. 86, 287–306.
Coint, N., Slagstad, T., Roberts, N., Marker, M., Røhr, T., Sørensen, B.E., 2015. The Late Mesoproterozoic Sirdal Magmatic Belt, SW Norway: relationships between magmatism and metamorphism and implications for Sveconorwegian orogenesis. Precambr. Res. 265, 57–77.
Collins, W., Beams, S., White, A., Chappell, B., 1982. Nature and origin of A-type granites with particular reference to southeastern Australia. Contrib. Miner. Petrol. 80, 189–200.
Deering, C.D., Bachmann, O., 2010. Trace element indicators of crystal accumulation in silicic igneous rocks. Earth Planet. Sci. Lett. 297, 324–331.
DePaolo, D.J., 1981. Neodymium isotopes in the Colorado Front Range and crust–mantle evolution in the Proterozoic. Nature 291 (5812), 193–196. https://doi.org/10.1038/291193a0.
Dostal, J., Dupuy, C., Carron, J., de Kerneizon, M.L.G., Maury, R., 1983. Partition coefficients of trace elements: application to volcanic rocks of St. Vincent, West Indies. Geochim. et Cosmochim. Acta 47, 525–533.
Drüppel, K., Elsäßer, L., Brandt, S., Gerdes, A., 2013. Sveconorwegian Mid-crustal Ultrahigh-temperature Metamorphism in Rogaland, Norway: U-Pb LA-ICP-MS Geochronology and Pseudosections of Sapphirine Granulites and Associated Paragneisses. J. Petrol.
Dudas, M., Schmitt, R., Harward, M., 1971. Trace element partitioning between volcanic plagioclase and dacitic pyroclastic matrix. Earth Planet. Sci. Lett. 11, 440–446.
Dunn, T., Sen, C., 1994. Mineral/matrix partition coefficients for orthopyroxene, plagioclase, and olivine in basaltic to andesitic systems: a combined analytical and experimental study. Geochim. Cosmochim. Acta 58, 717–733.
Eliasson, T., 1992. Magma genesis and emplacement characteristics of the peraluminous Sveconorwegian Bohus granite, SW Sweden. Geologiska Föreningen i Stockholm Förhandlingar 114, 452–455.
Eliasson, T., Ahlin, S., Petersson, J., 2003. Emplacement mechanism and thermobarometry of the Sveconorwegian Bohus granite, SW Sweden. GFF 125, 113–130.
Eliasson, T., Schöberg, H., 1991. U-Pb dating of the post-kinematic Sveconorwegian (Grenvillian) Bohus granite, SW Sweden: evidence of restitic zircon. Precambr. Res. 51, 337–350.
Falkum, T., 1982. Geologisk kart over Norge, berggrunnskart MANDAL - 1:250.000. Universitetsforlaget, Trondheim.
Falkum, T., Petersen, J., 1980. The Sveconorwegian orogenic belt, a case of late-Proterozoic plate-collision. Geol. Rundsch. 69, 622–647.
Flem, B., Grimstvedt, A., Slagstad, T., Skår, Ø., 2005. Bulkanalyse av Th og U i bergartsprøver med LA-ICP-MS. In: Metodebeskrivelse, NGU Rapport. 2005 Norges Geologiske Undersøkelse.
Frost, B.R., Barnes, C.G., Collins, W.J., Arculus, R.J., Ellis, D.J., Frost, C.D., 2001. A geochemical classification for granitic rocks. J. Petrol. 42, 2033–2048.
Fujimaki, H., Tatsumoto, M., Aoki, K.-I., 1984. Partition coefficients of Hf, Zr, and ree between phenocrysts and groundmasses. J. Geophys. Res. Solid Earth 89, B662–B672.
Garrido, C.J., Bodinier, J.-L., Burg, J.-P., Zeilinger, G., Hussain, S.S., Dawood, H., Chaudhry, M.N., Gervilla, F., 2006. Petrogenesis of mafic garnet granulite in the lower crust of the Kohistan paleo-arc complex (Northern Pakistan): implications for intra-crustal differentiation of island arcs and generation of continental crust. J. Petrol. 47, 1873–1914.
Glazner, A.F., Ussler III, W., 1988. Trapping of magma at midcrustal density discontinuities. Geophys. Res. Lett. 15, 673–675.
Goldstein, S.L., O'Nions, R.K., Hamilton, P.J., 1984. A Sm-Nd isotopic study of atmospheric dusts and particulates from major river systems. Earth Planet. Sci. Lett. 70, 221–236.
Goodge, J.W., Vervoort, J.D., 2006. Origin of Mesoproterozoic A-type granites in Laurentia: Hf isotope evidence. Earth Planet. Sci. Lett. 243, 711–731.
Green, T., Blundy, J., Adam, J., Yaxley, G., 2000. SIMS determination of trace element partition coefficients between garnet, clinopyroxene and hydrous basaltic liquids at 2–7.5 GPa and 1080–1200 C. Lithos 53, 165–187.
Grimes, C., Wooden, J., Cheadle, M., John, B., 2015. "Fingerprinting" tectono-magmatic provenance using trace elements in igneous zircon. Contrib. Miner. Petrol. 170, 46.
Hacker, B.R., Kelemen, P.B., Behn, M.D., 2011. Differentiation of the continental crust by relamination. Earth Planet. Sci. Lett. 307, 501–516.
Hanchar, J.M., Watson, E.B., 2003. Zircon saturation thermometry. Rev. Mineral. Geochem. 53, 89–112.
Hansen, E., Johansson, L., Andersson, J., Labarge, L., Harlov, D., Möller, C., Vincent, S., 2015. Partial melting in amphibolites in a deep section of the Sveconorwegian Orogen, SW Sweden. Lithos 236–237, 27–45.
Harrison, T.M., Watson, E.B., Aikman, A.B., 2007. Temperature spectra of zircon crystallization in plutonic rocks. Geology 35, 635–638.
Henderson, I.H., Ihlen, P.M., 2004. Emplacement of polygeneration pegmatites in relation to Sveco-Norwegian contractional tectonics: examples from southern Norway. Precambr. Res. 133, 207–222.
Hieronymus, C., Goes, S., 2010. Complex cratonic seismic structure from thermal models of the lithosphere: effects of variations in deep radiogenic heating. Geophys. J. Int. 180, 999–1012.
Hoskin, P.W.O., 2005. Trace-element composition of hydrothermal zircon and the alteration of Hadean zircon from the Jack Hills, Australia. Geochim. Cosmochim. Acta 69, 637–648.
Högdahl, K., Andersson, U.B., Eklund, O. 2004. The Transscandinavian Igneous Belt (TIB) in Sweden: a review of its character and evolution, Geological survey of Finland Espoo.
Jackson, S.E., Pearson, N.J., Griffin, W.L., Belousova, E.A., 2004. The application of laser ablation-inductively coupled plasma-mass spectrometry to in situ U-Pb zircon geochronology. Chem. Geol. 211, 47–69.
Jacobsen, S.B., Wasserburg, G.J., 1980. Sm-Nd isotopic evolution of chondrites. Earth Planet. Sci. Lett. 50, 139–155.
Jagoutz, O., Schmidt, M.W., 2013. The composition of the foundered complement to the continental crust and a re-evaluation of fluxes in arcs. Earth Planet. Sci. Lett. 371, 177–190.
Jensen, E., Corfu, F., 2016. The U-Pb age of the Finse batholith, a composite bimodal Sveconorwegian intrusion. Norw. J. Geol. 96, 171–178.
Jochum, K.P., Weis, U., Stoll, B., Kuzmin, D., Yang, Q., Raczek, I., Jacob, D.E., Stracke, A., Birbaum, K., Frick, D.A., 2011. Determination of reference values for NIST SRM 610–617 glasses following ISO guidelines. Geostand. Geoanal. Res. 35, 397–429.
Killeen, P., Heier, K., 1975a. A uranium and thorium enriched province of the Fennoscandian shield in southern Norway. Geochim. Cosmochim. Acta 39, 1515–1524.
Killeen, P.G., Heier, K.S., 1975b. Th, U, K, and heat production measurements in ten Precambrian granites of the Telemark area, Norway. Bulletin – Norges Geologiske Undersøkelse 59–83.
Kirkland, C., Slagstad, T., Johnson, T., 2018. Zircon as a metamorphic timekeeper: A case study from the Caledonides of central Norway. Gondwana Res. 61, 63–72.
Landenberger, B., Collins, W., 1996. Derivation of A-type granites from a dehydrated charnockitic lower crust: evidence from the Chaelundi Complex, Eastern Australia. J. Petrol. 37, 145–170.
Lugmair, G.W., Marti, K., 1978. Lunar initial 143Nd/144Nd: differential evolution of the lunar crust and mantle. Earth Planet. Sci. Lett. 39, 349–357.
Martin, H., 1987. Petrogenesis of Archaean trondhjemites, tonalites, and granodiorites from eastern Finland: major and trace element geochemistry. J. Petrol. 28, 921–953.
Matsui, Y., Onuma, N., Nagasawa, H., Higuchi, H., Banno, S., 1977. Crystal structure control in trace element partition between crystal and magma. Bulletin de la Societe Francaise de Mineralogie et de Cristallographie 100, 315–324.
McLelland, J.M., Selleck, B.W., Bickford, M.E., 2013. Tectonic evolution of the Adirondack Mountains and Grenville orogen inliers within the USA. Geosci. Can. 40, 318–352.
Menuge, J.F., 1988. The petrogenesis of massif anorthosites: a Nd and Sr isotopic investigation of the Proterozoic of Rogaland/Vest-Agder, SW Norway. Contrib. Miner. Petrol. 98, 363–373.
Menuge, J.F., Brewer, T.S., 1996. Mesoproterozoic anorogenic magmatism in southern Norway. Geol. Soc. London, Specl. Publicat. 112, 275–295.
Miller, C.F., McDowell, S.M., Mapes, R.W., 2003. Hot and cold granites? Implications of

zircon saturation temperatures and preservation of inheritance. Geology 31, 529–532.
Murakami, T., Chakoumakos, B.C., Ewing, R.C., Lumpkin, G.R., Weber, W.J., 1991. Alpha-decay event damage in zircon. Am. Mineral. 76, 1510–1532.
Möller, C., Andersson, J., Dyck, B., Antal Lundin, I., 2015. Exhumation of an eclogite terrane as a hot migmatitic nappe, Sveconorwegian orogen. Lithos 226, 147–168.
Nagasawa, H., Schnetzler, C.C., 1971. Partitioning of rare earth, alkali and alkaline earth elements between phenocrysts and acidic igneous magma. Geochim. Cosmochim. Acta 35, 953–968.
Nijland, T.G., Harlov, D.E., Andersen, T., 2014. The Bamble sector, south Norway: a review. Geosci. Front. 5, 635–658.
Okamoto, K., 1979. Geochemical study on magmatic differentiation of Asama volcano, central Japan. J. Geol. Soc. Jpn. 85, 525–535.
Pearce, J.A., Harris, N.B.W., Tindle, A.G., 1984. Trace-element discrimination diagrams for the tectonic interpretation of granitic rocks. J. Petrol. 25, 956–983.
Pedersen, S., Andersen, T., Konnerup-Madsen, J., Griffin, W.L., 2009. Recurrent Mesoproterozoic continental magmatism in south-central Norway. Int. J. Earth Sci. 98, 1151–1171.
Pedersen, S., Konnerup-Madsen, J., 2000. Geology of the setesdalen area, South Norway: Implications for the Sveconorwegian evolution of South Norway. Bull. Geol. Soc. Den. 46, 181–201.
Pedersen, S., Maaløe, S., 1990. The Iddefjord granite: geology and age. Norges geologiske undersøkelse Bulletin 417, 55–64.
Rayner, N., Stern, R.A., Carr, S.D., 2005. Grain-scale variations in trace element composition of fluid-altered zircon, Acasta Gneiss Complex, northwestern Canada. Contrib. Miner. Petrol. 148, 721–734.
Reid, F., 1983. Origin of the rhyolitic rocks of the Taupo Volcanic Zone, New Zealand. J. Volcanol. Geoth. Res. 15, 315–338.
Roberts, N.M.W., Slagstad, T., Parrish, R.R., Norry, M.J., Marker, M., Horstwood, M.S., 2013. Sedimentary recycling in arc magmas: geochemical and U-Pb–Hf–O constraints on the Mesoproterozoic Suldal Arc, SW Norway. Contrib. Miner. Petrol. 165, 507–523.
Scheiber, T., Viola, G., Bingen, B., Peters, M., Solli, A., 2015. Multiple reactivation and strain localization along a Proterozoic orogen-scale deformation zone: The Kongsberg-Telemark boundary in southern Norway revisited. Precambr. Res. 265, 78–103.
Schnetzler, C., Philpotts, J.A., 1970. Partition coefficients of rare-earth elements between igneous matrix material and rock-forming mineral phenocrysts—II. Geochim. Cosmochim. Acta 34, 331–340.
Schärer, U., Wilmart, E., Duchesne, J.-C., 1996. The short duration and anorogenic character of anorthosite magmatism: U-Pb dating of the Rogaland complex, Norway. Earth Planet. Sci. Lett. 139, 335–350.
Siégel, C., Bryan, S., Allen, C., Gust, D., 2018. Use and abuse of zircon-based thermometers: a critical review and a recommended approach to identify antecrystic zircons. Earth Sci. Rev. 176, 87–116.
Skår, Ø., 2002. U-Pb geochronology and geochemistry of early Proterozoic rocks of the tectonic basement windows in central Nordland, Caledonides of north-central Norway. Precambr. Res. 116, 265–283.
Slagstad, T., 2008. Radiogenic heat production of Archaean to Permian geological provinces in Norway. Norw. J. Geol. 88, 149–166.
Slagstad, T., Balling, N., Elvebakk, H., Midttømme, K., Olesen, O., Olsen, L., Pascal, C., 2009. Heat-flow measurements in Late Palaeoproterozoic to Permian geological provinces in south and central Norway and a new heat-flow map of Fennoscandia and the Norwegian-Greenland Sea. Tectonophysics 473, 341–361.
Slagstad, T., Roberts, N.M., Marker, M., Røhr, T.S., Schiellerup, H., 2013. A non-collisional, accretionary Sveconorwegian orogen. Terra Nova 25, 30–37.
Slagstad, T., Maystrenko, Y., Maupin, V., Gradmann, S., 2018a. An extinct, Late Mesoproterozoic, Sveconorwegian mantle wedge beneath SW Fennoscandia, reflected in seismic tomography and assessed by thermal modelling. Terra Nova 30, 72–77.
Slagstad, T., Roberts, N., Coint, N., Høy, I., Sauer, S., Kirkland, L., Marker, C., RØHR, M.S., Henderson, T.H.C., STORMOEN, I.A., SKÅR, M., SØRENSEN, Ø., BYBEE, G., 2018b. Magma-driven, high-grade metamorphism in the Sveconorwegian Province, southwest Norway, during the terminal stages of Fennoscandian Shield evolution. Geosphere 14, 861–882.
Slagstad, T., Roberts, N.M.W., Kulakov, E., 2017. Linking orogenesis across a supercontinent; the Grenvillian and Sveconorwegian margins on Rodinia. Gondwana Res. 44, 109–115.
Spencer, C.J., Roberts, N.M., Cawood, P.A., Hawkesworth, C.J., Prave, A.R., Antonini, A.S., Horstwood, M.S., 2014. Intermontane basins and bimodal volcanism at the onset of the Sveconorwegian Orogeny, southern Norway. Precambr. Res. 252, 107–118.
Stormoen, M.A., 2015. Synkinematic intrusion of granitoid sheets, with implications for molybdenite deposits in the Knaben Zone. Norges teknisk-naturvitenskapelige universitet Master of Science Master.
Sun, S.-S., McDonough, W., 1989. Chemical and isotopic systematics of oceanic basalts: implications for mantle composition and processes. Geol. Soc., London, Specl. Publicat. 42, 313–345.
Söderlund, U., Hellström, F.A., Kamo, S.L., 2008. Geochronology of high-pressure mafic granulite dykes in SW Sweden: tracking the P-T–t path of metamorphism using Hf isotopes in zircon and baddeleyite. J. Metamorph. Geol. 26, 539–560.
Söderlund, U., Isachsen, C.E., Bylund, G., Heaman, L.M., Jonathan Patchett, P., Vervoort, J.D., Andersson, U.B., 2005. U–Pb baddeleyite ages and Hf, Nd isotope chemistry constraining repeated mafic magmatism in the Fennoscandian Shield from 1.6 to 0.9 Ga. Contribut. Mineral. Petrol 150, 174.
Taylor, S.R., McLennan, S.M. 1985. The continental crust: its composition and evolution.
Tual, L., Pitra, P., Möller, C., 2017. P-T evolution of Precambrian eclogite in the Sveconorwegian orogen, SW Sweden. J. Metamorph. Geol. 35, 493–515.
van Achterbergh, E., Ryan, C.G., Jackson, S.E., Griffin, W.L., 2001. Appendix 3, Data reduction software for LA-ICP-MS. Sylvester, P.J. (Ed.), Laser Ablation-ICPMS in the Earth Sciences: Principles and Applications, Mineralogical Association of Canada Short Course Series 29, 239–243.
Vander Auwera, J., Bogaerts, M., Liégeois, J.-P., Demaiffe, D., Wilmart, E., Bolle, O., Duchesne, J.C., 2003. Derivation of the 1.0–0.9 Ga ferro-potassic A-type granitoids of southern Norway by extreme differentiation from basic magmas. Precambr. Res. 124, 107–148.
Vander Auwera, J., Bolle, O., Bingen, B., Liégeois, J.-P., Bogaerts, M., Duchesne, J.-C., De Waele, B., Longhi, J., 2011. Sveconorwegian massif-type anorthosites and related granitoids result from post-collisional melting of a continental arc root. Earth-Sci. Rev. 107, 375–397.
Vander Auwera, J., Bolle, O., Dupont, A., Pin, C., Paquette, J.-L., Charlier, B., Duchesne, J.C., Mattielli, N., Bogaerts, M., 2014. Source-derived heterogeneities in the composite (charnockite-granite) ferroan Farsund intrusion (SW Norway). Precambr. Res. 251, 141–163.
Viola, G., Henderson, I.H.C., Bingen, B., Hendriks, B.W.H., 2011. The Grenvillian-Sveconorwegian orogeny in Fennoscandia: Back-thrusting and extensional shearing along the “Mylonite Zone”. Precambr. Res. 189, 368–388.
Watson, E.B., Harrison, T.M., 1983. Zircon saturation revisited: temperature and composition effects in a variety of crustal magma types. Earth Planet. Sci. Lett. 64, 295–304.
Welin, E., 1994. Isotopic investigations of Proterozoic igneous rocks in south-western Sweden. GFF 116, 75–86.
Whalen, J.B., Currie, K.L., Chappell, B.W., 1987. A-type granites: geochemical characteristics, discrimination and petrogenesis. Contrib. Miner. Petrol. 95, 407–419.
Whattam, S.A., 2018. Primitive magmas in the early Central American volcanic arc system generated by plume-induced subduction initiation. Front. Earth Sci. 6.
Whitney, J.A., 1988. The origin of granite: the role and source of water in the evolution of granitic magmas. Geol. Soc. Am. Bull. 100, 1886–1897.
Wiedenbeck, M., Allé, P., Corfu, F., Griffin, W., Meier, M., Oberli, F.V., von Quadt, A., Roddick, J., Spiegel, W., 1995. Three natural zircon standards for U-Th-Pb, Lu-Hf, trace element and REE analyses. Geostand. Newslett. 19, 1–23.
Wiest, J.D., Jacobs, J., Ksienzyk, A.K., Fossen, H., 2018. Sveconorwegian vs. Caledonian orogenesis in the eastern Øygarden Complex, SW Norway – Geochronology, structural constraints and tectonic implications. Precambr. Res.
Zhao, J.-L., Qiu, J.-S., Liu, L., Wang, R.-Q., 2016. The Late Cretaceous I- and A-type granite association of southeast China: implications for the origin and evolution of post-collisional extensional magmatism. Lithos 240–243, 16–33.
Zhao, X.-F., Zhou, M.-F., Li, J.-W., Wu, F.-Y., 2008. Association of Neoproterozoic A- and I-type granites in South China: implications for generation of A-type granites in a subduction-related environment. Chem. Geol. 257, 1–15.
Åhäll, K.-I., Connelly, J.N., 2008. Long-term convergence along SW Fennoscandia: 330m. y. of Proterozoic crustal growth [Precam Res 161 (2008) 452–472]. Precambr. Res. 163, 402–421.